Bose-Einstein Condensates in asymmetric quasi-periodic lattices

Miguel Paço
Mestrado em Física
Departamento de Física e Astronomia
2023

Orientador
Prof. Dr. Augusto Rodrigues, Professor Auxiliar, Faculdade de Ciências da Universidade do Porto

“ My light shines out as a Golden Path. ”

Leto II Atreides in Children of Dune, written by Frank Herbert

Acknowledgements

This thesis was made with the support of the Fundação para a Ciência e a Tecnologia under the contract PTDC/FIS-OUT/3882/2020.

I'd like to begin by recognizing how this past year has truly changed the way i look at physics and how it's done, and that could not have been possible without my great supervisor who was always ready to hear my questions and provided with so much material to read and learn, suggestions and corrections to this work.

My family has also been very important throughout not only this year but my entire academic career, with my parents always encouraging me to pursue what i wanted to study and supporting me in that endeavour, and both my siblings that are always there to annoy me and help me at the same time.

I also want to thank every friend that this last year i sat down to have lunch or a cup of coffee, went to the movies or just hung out, as you kept me going and in touch with everything outside of this. In particular i need to thank my oldest friend and also coach Tiago, that besides all this also encouraged me to restart practicing taekwondo, which has been vital for my well being.

Finally i need to thank my biggest support and life partner, my girlfriend Francisca, that has been encouraging me through the difficult research and writing process, and is always there to help me relax and keep me going. She is the sweetest and most thoughtful person i know.

UNIVERSIDADE DO PORTO

Abstract

Faculdade de Ciências da Universidade do Porto
Departamento de Física e Astronomia

MSc. Physics

Bose-Einstein Condensates in asymmetric quasi-periodic lattices

by Miguel Paço

We consider a Bose-Einstein Condensate in an asymmetric quasi periodic lattice formed by two sublattices whose periods are incommensurate by using a Rational Approximation of the golden ratio. We show that when dealing with a non interacting BEC, breaking the symmetry of the potential has no effect on the mobility edge and memory effect of the energy spectrum of the system manifested via gaps in the energy, but it breaks the symmetry of the centers of mass of the linear states, meaning that ground states for the condensate are no longer symmetric or anti symmetric as was the case for the symmetric potential. We find on the linear ground state a mobility edge for the amplitude v_2 of one of the waves of the potential at amplitudes $v_1 = 0.8; \quad v_2 = 0.6$. Through linear stability analysis with the Bogoliubov-de Gennes equations we were able to find localized excitations rising from stable and unstable non linear states. For unstable states we also calculated the time evolution of the state perturbed by the localized excitation. For the Condensate with repulsive particle interaction we were able to determine the time frame of decay of the Condensate at around 620 units of time, or 1.98τ. For the Condensate with attractive particle interaction the time frame of decay determined was 600 units of time, or 16.13τ.

UNIVERSIDADE DO PORTO

Resumo

Faculdade de Ciências da Universidade do Porto
Departamento de Física e Astronomia

Mestrado em Física

Condensados de Bose-Einstein em redes assimétricas quase periódicas

por Miguel Paço

Consideramos um Condensado de Bose-Einstein em uma rede assimétrica quase periódica, formada por duas sub redes cujos períodos são incomensuráveis usando uma aproximação racional da razão de ouro. Mostramos que ao lidar com um Condensado sem interação entre partículas, quebrar a simetria do potencial não tem qualquer efeito na mobility edge e no efeito de memória existente no espetro de energia do sistema, mas quebra a simetria dos centros de massa dos estados lineares, significando que ao contrário do que acontecia para o condensado em um potencial simétrico os estados deixam de ser necessariamente simétricos ou anti simétricos. Determinamos para o estado fundamental linear a mobility edge para a amplitude v_2 de uma das ondas constituintes do potencial, nos valores de amplitude $v_1 = 0.8; \quad v_2 = 0.6$. Através de análise de estabilidade linear usando as equações de Bogoliubov-de Gennes encontramos oscilações localizadas que se formam a partir de estados não lineares deslocalizados, tanto estáveis como instáveis. Para os estados instáveis calculamos a propagação temporal do Condensado perturbado pela oscilação localizada, onde no Condensado com interação repulsiva entre partículas determinamos que o intervalo de tempo de decaimento é por volta de 620 unidades de tempo, ou 1.98τ, enquanto que para o condensado com interação atrativa entre partículas esse decaimento ocorreu pelas 600 unidades de tempo, ou 16.13τ.

Contents

List of Figures

Glossary

BEC	Bose Einstein Condensate
GPE	Gross Pitaevskii Equation
BdG	Bogoliubov de Gennes
IPR	Inverse Participation Ratio
LSA	Linear Stability Analysis
ME	Mobility Edge
RA	Rational Approximation

Chapter 1

Introduction

The existence and propagation of matter waves in Bose-Einstein Condensates is one of the most well-studied problems in this area of Condensed Matter Physics [1–11]. Solitons and Phonons are two types of these matter waves that have been studied ever since the first synthetization of a BEC in 1998. This thesis will delve a bit further into this problem and other, trying to obtain localized matter waves from delocalized states and by evaluating the effects on the linear states of the condensate of breaking the symmetry of the quasi periodic potential. We will start by giving a theoretical foundation of BECs in chapter 2, and in chapter 3 we will look at the effects of trapping a Condensate in different types of potentials, namely periodic and quasi periodic ones. After a detailed description of the numerical methods used throughout this thesis is given in chapter 4 we will look at the different results obtained. We will start by evaluating the effect of breaking the symmetry of the quasi periodic potential, followed by the determination of the mobility edge for the amplitude of the waves of the potential of this system. After it has been obtained we are going to perform linear stability analysis via the Bogoliubov-de Gennes equations on the various delocalized nonlinear states obtained, and depending on the result of the analysis we are going to look for localized perturbations on stable and unstable states. For the unstable ones we are also going to calculate the time evolution of the nonlinear state after it has been perturbed, in order to evaluate the time frame of the instability and the validity of the linear stability analysis, since Bogoliubov-de Gennes analysis is valid on the linear limit.

Chapter 2

Bose-Einstein Condensates

The Bose-Einstein Condensate has been an object of theoretical study ever since 1924, after its first prediction by Albert Einstein [12] based on the quantum statistical theory developed by Satyendra Bose the previous year [13]. Taking the idea to treat Electromagnetic Waves as a gas of identical particles, Einstein applied the same thought to gases of particles with integer spin and some atoms (such as Helium-4). When such a gas is cooled to a low enough temperature (the critical Temperature T_c), a phase transition can be triggered, driven by Quantum Statistical Mechanics. On this transition the gas particles occupy the lowest quantum state, forming a new state of matter. This is possible due to the fact that bosons follow Bose-Einstein statistics. The BEC is one of the few quantum systems where the effects are noticeable on a macroscopic scale. Due to experimental constraints it was not until 1995 that Eric Cornell and Carl Wieman first produced a condensate in a lab, by cooling a gas of rubidium atoms to 170 nanokelvin [14]. After that first moment of synthesis much work has been done in the study of BECs. A rather complete review of these studies was done by Dalfovo et al. in 1998 [15] and it joins various topics such as the stability limit for a Condensate with attractive forces, the Thomas Fermi limit for large N and repulsive forces, the validity of the mean field theory and some corrections to it, as well as dynamics of excitations of the condensate. The propagation of solitons formed by BECs is also a big area of study, being one of the most evident nonlinear phenomena that can be observed, since their formation is directly dependant on the balance of the effects of diffraction and the nonlinear self focusing (or self defocusing, depending on the type of particle interaction) that rises from particle interactions. Theoretically it appeared for the first time in [1], where by solving the GPE on a highly asymmetrical trap it was found that the BEC can behave like a quasiparticle. For experimental evidence we can

look at the work done by Khaykovich et al. [7], which by tuning the interaction of the BEC through Feshbach resonance were able to observe the propagation of a soliton over a macroscopic distance. On BECs with attractive particle interaction trains of solitons have been observed [6], where up to ten solitons were observed to travel through an axial potential, with repulsive interaction among consecutive solitons of the train. For a BEC with repulsive particle interaction a dark soliton (or kink state) can be formed, and in [8] we can see the study of the equation of motion and stability analysis for such waves, and experimental evidence in [2] and the testing of dynamics.

2.1 Gross-Pitaevskii Equation

Since the particles all occupy the same state, they can be described by the same macroscopic wavefunction $\psi(\vec{r},t)$, and on a dilute enough BEC it is possible to describe it using the Gross-Pitaevskii Equation [16], which is a nonlinear Schrödinger Equation. This nonlinearity arises when we consider interactions between the particles inside the gas, and they can be both repulsive or attractive. In order to arrive at this Equation we can begin by writing the many body Hamiltonian of a gas of interacting particles in second quantization, which for N particles subject to an external potential $V(\vec{r})$ is given by:

$$\hat{H} = \int d\vec{r}\hat{\Psi}^\dagger(\vec{r})\left(-\frac{\hbar^2}{2m}\nabla^2 + V(\vec{r})\right)\hat{\Psi}(\vec{r}) + \frac{1}{2}\int d\vec{r}d\vec{r}'\hat{\Psi}^\dagger(\vec{r})\hat{\Psi}^\dagger(\vec{r}')U(\vec{r}-\vec{r}')\hat{\Psi}(\vec{r}')\hat{\Psi}(\vec{r}). \tag{2.1}$$

Where $\hat{\Psi}(\vec{r})$ and $\hat{\Psi}^\dagger(\vec{r})$ are the boson field annihilation and creation operators, $V(\vec{r})$ is the external potential added onto the BEC and $U(\vec{r}-\vec{r}')$ is the interaction potential between particles, that we are assuming only depends on the distance between them. The commutation relations for the boson field operators are the following:

$$\left[\hat{\Psi}(\vec{r},t),\hat{\Psi}^\dagger(\vec{r}',t)\right] = \delta(\vec{r}-\vec{r}'),\left[\hat{\Psi}(\vec{r},t),\hat{\Psi}(\vec{r}',t)\right] = \left[\hat{\Psi}^\dagger(\vec{r},t),\hat{\Psi}^\dagger(\vec{r}',t)\right] = 0. \tag{2.2}$$

With this we can derive the final wavefunction by use of the Heisenberg equation:

$$i\hbar\frac{\partial}{\partial t}\hat{\Psi}(\vec{r},t) = \left[\hat{\Psi}(\vec{r},t),\hat{H}\right], \tag{2.3}$$

and we are going to obtain:

$$i\hbar\frac{\partial}{\partial t}\hat{\Psi}(\vec{r},t) = \left[-\frac{\hbar^2}{2m}\nabla^2 + V(\vec{r}) + \int d\vec{r}'\hat{\Psi}^\dagger(\vec{r}')U(\vec{r}-\vec{r}')\hat{\Psi}(\vec{r}')\right]\hat{\Psi}(\vec{r}). \tag{2.4}$$

Now we must think about the interaction term. Previously it was said that this equation can be applied to a dilute enough Condensate, so a good approximation is made if we consider the only collisions that occur to be between two particles, characterized by a single parameter, the *s*-wave scattering length. Denoting this length as a, and is negative for an attractive particle interaction and is positive for a repulsive particle interaction. With this in mind the following substitution can be made for the potential:

$$U(\vec{r}-\vec{r}') = g\delta(\vec{r}-\vec{r}'), \tag{2.5}$$

where g is given by $\frac{4\pi\hbar^2 a}{m}$. This is the potential obtained by looking only at the lowest energy wave on a partial wave expansion [17]. Before we complete the calculation of our wavefunction we must take into consideration that when Condensation occurs the number of atoms in the ground state, N_0, will be very large, meaning that on a macroscopic level the states with N_0 and $N_0 \pm 1$ will correspond to the same physical configuration, so the field operators may be decomposed into an expectation term and a fluctuation term, this being the Bogoliubov prescription [16]:

$$\hat{\Psi} = \hat{\Phi} + \delta\Psi, \quad \hat{\Psi}^\dagger = \hat{\Phi}^\dagger + \delta\Psi^\dagger. \tag{2.6}$$

The term $\hat{\Phi}$ is a function defined as the expected value of the field operator $\hat{\Phi} = \langle\hat{\Psi}\rangle$. Its modulus is the condensate density $n_0 = |\hat{\Phi}|^2$ and the function $\Phi(\vec{r},t)$ can be regarded as a classical field and is an order parameter (because $n_0 \approx 0$ when $T > T_c$, and $n_0 \neq 0$ when $T \leq T_c$) , commonly referred to as the wavefunction of the condensate. With this in mind we can substitute our expanded field operators into the previous equation, and since we want our condensate to be dilute and at low temperature the quantum fluctuations can be neglected. Our substitution will finally yield the Gross-Pitaevskii Equation:

$$i\hbar\frac{\partial}{\partial t}\psi(\vec{r},t) = \left[-\frac{\hbar^2}{2m}\nabla^2 + V(\vec{r}) + g|\psi(\vec{r},t)|^2\right]\psi(\vec{r},t). \tag{2.7}$$

In our derivation process many approximations were made, so it must be noted that this equation is valid when the scattering length is much smaller than the average distance between particles and when the number of particles is much larger than 1. The number of atoms N may also be defined as $\mathcal{N} = \int dx|\psi|^2$.

2.2 Ground State

Now that we have an equation for the state of the Condensate we can for example obtain the ground state of the condensate. This can be done simply through the choice of the correct ansatz, by writing our wavefunction as $\Phi(\vec{r},t) = \phi(\vec{r})e^{-\frac{i\mu t}{\hbar}}$, where μ is the chemical potential and ϕ is real and normalized to the number of particles $\int d\vec{r}|\phi|^2 = N$. Substituting this solution in the GPE we will obtain:

$$\mu\phi(\vec{r}) = \left[-\frac{\hbar^2}{2m}\nabla^2 + V(\vec{r}) + g|\phi(\vec{r})|^2\right]\phi(\vec{r}). \tag{2.8}$$

This is, as said before, a nonlinear Schrödinger equation, where the nonlinear term comes from the interaction between particles. When there are no interactions this reduces simply to a regular Schrödinger equation for a single particle, and when harmonic confinement is present, the ground state solution becomes a Gaussian function. For different families of potentials the GPE may be solved numerically. For weak nonlinearity the solutions first branch out from the Gaussian profile.

2.3 Dimension Reduction of BEC

So far we have been working with a three dimensional and isotropic condensate, but it will be useful later on to understand how one may model the Condensate as if it only were one or two dimensional. This can be done by submitting the Condensate to a harmonic trapping potential. With this in mind the external potential can be written as:

$$V(\vec{r},t) = V_{trap}(\vec{r},t) + V_{lattice}(\vec{r},t), \tag{2.9}$$

where $V_{trap}(\vec{r},t) = \frac{m}{2}\left(\omega_x^2x^2 + \omega_y^2y^2 + \omega_z^2z^2\right)$ is the harmonic trapping potential and $V_{lattice}(\vec{r},t)$ is any other lattice potential present in the setup, that may be periodic or quasi-periodic, which as we will see ahead will be the case for this thesis. In order to model the Condensate as if it were one dimensional we need to set each of the axial frequencies $\omega_x,\omega_y,\omega_z$ adequately, which in this case will mean that $\omega_y = \omega_z = \omega_{yz} \gg \omega_x$. Defining the characteristic length of each dimension as the characteristic harmonic oscillator length $l_i = \sqrt{\frac{\hbar}{m\omega_i}}, \quad i \in \{x,y,z\}$ we see that with these frequencies we will have $l_x \gg l_{yz}$, where $l_{yz} = l_y = l_z$. This difference in characteristic length is what allows us to model the Condensate as if it were one dimensional [1]. In order to calculate the effect of this change in

dynamic on the nonlinear equation we are solving it is useful first to rescale our variables such that we work with a adimensional equation. In order to do this we must redefine our variables and potential in terms of the fundamental constants of the problem in the following manner:

$$t' = \omega_{yz} t \quad \vec{r}' = \frac{\vec{r}}{l_{yz}} \quad \psi'(\vec{r}', t') = l_{yz}^{\frac{3}{2}} \psi(\vec{r}, t) \quad V'(\vec{r}', t') = \frac{1}{\hbar \omega_{yz}} V(\vec{r}, t). \tag{2.10}$$

And substituting these new variables and dropping the ' we will obtain the following adimensional equation:

$$i \frac{\partial}{\partial t} \psi(\vec{r}, t) = \left[-\frac{1}{2} \nabla^2 + V(\vec{r}) + g_{3D} |\psi(\vec{r}, t)|^2 \right] \psi(\vec{r}, t), \tag{2.11}$$

where $g_{3D} = \frac{4\pi a}{l_{yz}}$. The potential now takes the form $V(\vec{r}, t) = \frac{1}{2} \left(\frac{\omega_x}{\omega_{yz}} x^2 + \rho^2 \right) + V_{lattice}(\vec{r}, t)$, where $\rho^2 = y^2 + z^2$. Due to our previous choice of longitudinal frequencies we will have $\frac{\omega_x}{\omega_{yz}} \ll 1$, and because of this trapping we may assume the wavefunction to have a separable solution of the form $\psi(\vec{r}, t) = \Phi(\rho)\Psi(x, t)$ and that the tight confinement in the y, z directions makes it so we can describe the radial function $\Phi(\rho)$ as a solution to the 2D quantum harmonic oscillator $\nabla^2 \Phi + \Phi - r^2 \Phi = 0$ [18]. Assuming the ground state solution $\Phi(\rho) = \frac{1}{\sqrt{\pi}} e^{-\frac{\rho^2}{2}}$ we need to multiply the equation by Φ^* and integrate in $d\rho$ to eliminate the transverse dependency. After that we will arrive at the effective one dimensional equation we solve for the Condensate:

$$i \frac{\partial}{\partial t} \Psi(x, t) = \left[-\frac{1}{2} \frac{\partial^2}{\partial x^2} + V(x) + g_{1D} |\Psi(x, t)|^2 \right] \Psi(x, t), \tag{2.12}$$

where $g_{1D} = \frac{2a}{l_{yz}}$. Now it is again important to adimensionalize our equation, and this time we only need to rescale our wavefunction as $\psi(x, t) = \sqrt{g_{1D}} \Psi(x, t)$ where we will finally obtain the adimensional effective one dimensional GPE:

$$i \frac{\partial}{\partial t} \psi(x, t) = \left[-\frac{1}{2} \frac{\partial^2}{\partial x^2} + V(x) + g |\psi(x, t)|^2 \right] \psi(x, t). \tag{2.13}$$

In this equation the parameter $g = \pm 1$, where $g = 1$ refers to a positive scattering length of the particles and $g = -1$ refers to a negative scattering length.

Chapter 3

BECs in Potentials

3.1 BECs in Periodic Potentials

Now that we have an understanding of the mechanism of Bose-Einstein condensation, we want to look at the effects of submitting the condensate to certain types of potentials. Let's start by looking at a BEC in a periodic potential. In this and the following chapters we will be working with a one dimensional BEC, whose equation is the one obtained in the previous section. With this in mind let us look at some properties of BECs in periodic potentials.

3.1.1 Periodic Potentials

First, we must define what a periodic function is. That can be done in a simple manner. A function $f(x)$ is periodic if there exists a quantity P, the period, such that for any x:

$$f(x+P) = f(x). \tag{3.1}$$

Solving the Schrödinger equation in a periodic potential is a very well understood problem. Most physical problems in metals and semi metals involve a periodic potential, corresponding to a crystal lattice. These problems are made easier by use of the Bloch Theorem, that states that the wavefunction of a particle moving in a periodic potential is a Bloch function (also called Bloch state) $\psi(x)$ composed of a plane wave e^{ikx} and a periodic factor $u(x)$, that has the same periodicity as the underlying potential:

$$\psi_k(x) = u_k(x)e^{ikx}; \quad u_k(x+P) = u_k(x). \tag{3.2}$$

When talking about this Theorem it is also important to introduce Wannier states, which are also used when describing electrons in crystal lattices. They can be obtained the following way from the Bloch states:

$$\phi_R(x) = \frac{1}{\sqrt{N}} \sum_k e^{-ikR} \psi_k(x), \tag{3.3}$$

where the sum occurs over every k in the Brillouin Zone, R is any vector of the lattice and N is the number of primitive cells in the crystal. If our problem is on a one dimensional lattice any vector of this lattice can be written as $R_n = n\hat{a}$, where $\hat{a}$ is the primitive vector and each value of n will correspond to a different cell. In this case the Wannier functions can be written in a different, more concise notation, this notation being $\phi_{R_n} = |n\rangle$. $|n\rangle$ corresponds then to the Wannier function of the n^{th} cell.

Besides looking at these extended ground states we may also look at the formation of solitons in BECs in periodic potentials. One such study is given in [18], where the authors first look at the band gaps from the noninteracting condensate that arise from solving the Gross-Pitaevskii equation using the Bloch theorem. Later by adding particle interaction they obtain nonlinear Bloch waves and look at the localized solutions in the band gaps of the spectrum, the so called gap solitons, and evaluate their stability.

3.2 BECs in Quasi Periodic Potential

Having looked at some relevant aspects of a BEC in a periodic potential we want to take it a step further and look now at the dynamic obtained by using a quasi periodic potential, that has slightly different properties and alters the way the BEC behaves. First we need to understand what is a quasi periodic potential, understand some general models that exist in quasi periodic potentials, and then turn our attention specifically to BECs, where we can look at the mobility edge and some nonlinear dynamics.

3.2.1 Quasi Periodic Potentials

Although the class of potentials that we will use is called "Quasi Periodic Potentials", on a mathematical sense they most closely resemble Almost Periodic Functions [19], so it is helpful to define what they are. They can be seen as a generalisation of periodic functions and were first studied by Harald Bohr. Such a function can be thought of as a function that is periodic to an arbitrary degree of precision within some almost-period,

that is related to the intended precision. Though there are many different ways to express this same condition we will stick to the one first given by Bohr. And so, a function $f(x)$ is Almost Periodic if there is, for every value $\epsilon > 0$, a length $L(\epsilon)$ such that in every interval $[A, A + L(\epsilon)]$ there is an associated ϵ-translation number $\tau(\epsilon)$ such that:

$$|f(x + \tau(\epsilon)) - f(x)| \leq \epsilon. \tag{3.4}$$

Another equivalent way to say it is if a function is almost periodic then it can be approximated to any degree of accuracy by a trigonometric potential $t_\epsilon = \sum_n e^{i\lambda_n x}$

$$|f(x) - t_\epsilon(x)| \leq \epsilon. \tag{3.5}$$

By the first definition it is easy to see that regular periodic functions also fall under the umbrella of Almost Periodic ones, simply by making the function $\tau(\epsilon) = \tau$ where τ is the period of the function and ϵ can be simply set to 0. Since we're working in a one dimensional system it is useful to understand how we may create such a potential in one dimension. A simple and effective way is to superimpose two monochromatic standing waves $V_1 = v_1 \cos(2x)$, $V_2 = v_2 \cos(2\alpha x + \phi)$ whose periods are incommensurate, which means that α must be irrational. If they are not incommensurate we can write $\alpha = \frac{a}{b}$, which means that the waves will have a common period in the following manner:

$$V(x + b\pi) = v_1 \cos(2x + 2b\pi) + v_2 \cos(2\alpha x + 2a\pi + \phi) = V(x), \tag{3.6}$$

which means that the potential is periodic. If, as said before, the periods are incommensurate then it is no longer possible to find a common period, and we can instead expand our potential in the following manner:

$$V(x) = \frac{v_1}{2} e^{2ix} + \frac{v_1}{2} e^{-2ix} + \frac{v_2}{2} e^{i(2\alpha x + \phi)} + \frac{v_2}{2} e^{-i(2\alpha x + \phi)}, \tag{3.7}$$

which fits our definition of almost periodic function, where in this case we can set ϵ to zero. Under circumstances that we will explain further ahead it is possible to substitute the value of the irrational number α by a Rational Approximation of it, $\alpha \approx \frac{M}{N}$. The details of this Approximation will depend on the choice of irrational number. For the Golden Ratio $\frac{1+\sqrt{5}}{2}$ a way to find such an approximation is to divide two consecutive terms of the Fibonacci sequence.

3.2.2 Quasi Periodic Systems

The interest in studying systems that exist in quasi periodic potentials came decades after the mathematical description of these functions and nowadays has made its way to physics, with one of its first instances being the discussion of an atomic structure with almost periodic translation order [20]. In fact nowadays many structures studied in physics are almost periodic, like in 1D the superposition of two incommensurate potentials, in 2D the so called quasi crystals or Moiré lattices, obtained by imposing two lattices and twisting one of them, The most famous example is twisted bilayer graphene [21], where many exotic properties can be observed including superconductivity.

3.2.3 Localization in Quasi Periodic Potentials

Anderson localization [22] is a phenomenon much studied in Solid State Physics and Many Body Quantum Physics and it is a phenomenon regarding the localization of quantum waves in the presence of disorder. It has been observed in many different BEC systems and its observation has become more common as better experimental methods are developed, for example in a BEC in a bichromatic lattice [23], where by varying the amplitude and wavelength of a non interacting BEC a transition of localized to delocalized state is triggered, on a 3D random potential [24] where the expansion of a BEC with repulsive interactions is analyzed depending on the strength of a random potential and on other quasi periodic potentials [25], where a BEC produced by cooling a cloud of Potassium atoms, made to be non-interacting through Feshbach resonance, is observed to become localized as the amplitude of the quasi periodic potential is increased. In [26] the BEC is instead produced by evaporating the Rubidium atoms of a Potassium-Rubidium gas and Feshbach resonance is used during this evaporation to produce either a Localized or delocalized BEC. One of the more important instances of a BEC in a quasi periodic potential comes in the form of the Aubry-André model [25, 27]. This model is very useful in order to study the localization properties of the BEC, that in this case depend on the strength of the potential. Localization in this model has been observed experimentally [28] and it can be defined by the Hamiltonian [27]:

$$H = -J\sum(|n\rangle\langle n+1| + |n+1\rangle\langle n|) + \lambda\sum_n \cos(2\pi\beta n)|n\rangle\langle n|, \tag{3.8}$$

where $|n\rangle$ is the Wannier state at site n, J is the hopping strength, λ the potential strength and β, which is commonly chosen to be an irrational number (frequently $\frac{1}{\varphi}$, where φ is the golden ratio $\varphi = \frac{1+\sqrt{5}}{2}$) determines the periodicity of the potential. The irrationality of the periods make it so there is a critical value of the potential strength for which there is a localization transition in the condensate. The existence of this critical value of the amplitude of the trapping potential tells us that there is a mobility edge for this system, a well defined value that separates between localized and delocalized states of the condensate. This system bears some resemblance to the one being studied in this thesis, hence its importance.

Chapter 4

Numerical Methods

The present chapter will be dedicated to explaining in detail all the numerical methods used in this thesis to obtain linear and nonlinear states of the condensate, energy spectra and elementary oscillations. Besides the mathematical formulation an explanation of its use will also be given.

4.1 Linear State of GPE

This first method is used in order to calculate eigenvalues and eigenvectors of the linearized version of the GPE, that models a boson gas without inter particle interaction. This is the first method used to obtain the ground state. Since we want the eigenvalues and eigenvectors this means we must discretize the equation according to our lattice. Starting with the linearized adimensional GPE we want to solve for the ground state the following:

$$\mu\psi(x) = \left[-\frac{1}{2}\frac{\partial^2}{\partial x^2} + V(x)\right]\psi(x). \tag{4.1}$$

We will use as external potential the quasi periodic potential discussed in the previous chapter, where for irrational number we will use the golden ratio $\varphi = \frac{1+\sqrt{5}}{2}$ and as said previously a rational approximation of this number $\varphi \approx \frac{M}{N}$ will be used. The justification for these choices will be given further ahead in this document. As such, the potential will have the form $V(x) = v_1\cos(2x) + v_2\cos\left(2\frac{M}{N}x + \phi\right)$, and the domain of our condensate will be $x \in \left[-\frac{N\pi}{2}, \frac{N\pi}{2}\right]$. We will divide the domain into N_x pieces such that the position in the lattice may be expressed as $x_i = i\Delta x - \frac{N\pi}{2}, i \in [0, N_x - 1]$, where $\Delta x = \frac{N\pi}{N_x}$. For the discretization of the Laplacian we will use the second order central finite difference method:

$$\nabla^2\psi_i = \frac{\psi_{i-1} - 2\psi_i + \psi_{i+1}}{\Delta x^2}, \tag{4.2}$$

where $\psi_i = \psi(x_i)$. In our thesis we will work with periodic boundary conditions $\psi\left(-\frac{N\pi}{2}\right) = \psi\left(\frac{N\pi}{2}\right)$, which will change the laplacian term of the first and last points of the domain. In order to discretize the potential we can simply write

$$V_i = V(x_i) = v_1\cos(2x_i) + v_2\cos\left(2\frac{M}{N}x_i + \phi\right). \tag{4.3}$$

And with this in mind we can write the discretized equation in the following way:

$$-\frac{1}{2\Delta x^2}\psi_{i-1} + \left(V_i + \frac{1}{\Delta x^2}\right)\psi_i - \frac{1}{2\Delta x^2}\psi_{i+1} = \mu\psi_i, \tag{4.4}$$

which can be seen simply as an eigenvalue problem of a matrix equation, and can be rewritten in the following way:

$$H\psi = \mu\psi, \tag{4.5}$$

where H is a sparse matrix with three nonzero diagonals and two extra terms to account for the periodic boundary conditions. The terms of the matrix are the following:

$$\begin{aligned} H_{j,j} &= V_j + \frac{1}{\Delta x^2}, \\ H_{j,j+1} = H_{j+1,j} &= -\frac{1}{2\Delta x^2}, \\ H_{1,N_x} = H_{N_x,1} &= -\frac{1}{2\Delta x^2}. \end{aligned} \tag{4.6}$$

After we solve for the eigenvalues and eigenvectors it is important that we understand what we have just calculated. This method is used to determine the ground state of a Bose-Einstein Condensate with no particle interaction, and thus both the eigenvector and eigenvalue must be related to that. Firstly the eigenvector is the wavefunction of the BEC, where each point ψ_i is the value of the wavefunction on the i^{th} point of the domain, and the eigenvalue is the chemical potential, that came from substituting the stationary ansatz. It is common for this linear state to be normalized such that $\mathcal{N} = \int dx|\psi|^2 = 1$. With this formulation the problem becomes simply one of solving it numerically. When writing Python code, due to the fact that this matrix is sparse, the sparse linear algebra module becomes useful. We provide as an example the linear ground state obtained by this method for the parameters $v_1 = 0.8; v_2 = 0.65; \phi = \sqrt{2}; \varphi \approx \frac{233}{144}$, where this approximation

for the golden ratio $\varphi = \frac{1+\sqrt{5}}{2}$ comes from dividing two consecutive terms of the Fibonacci sequence, as referred in the previous chapter.

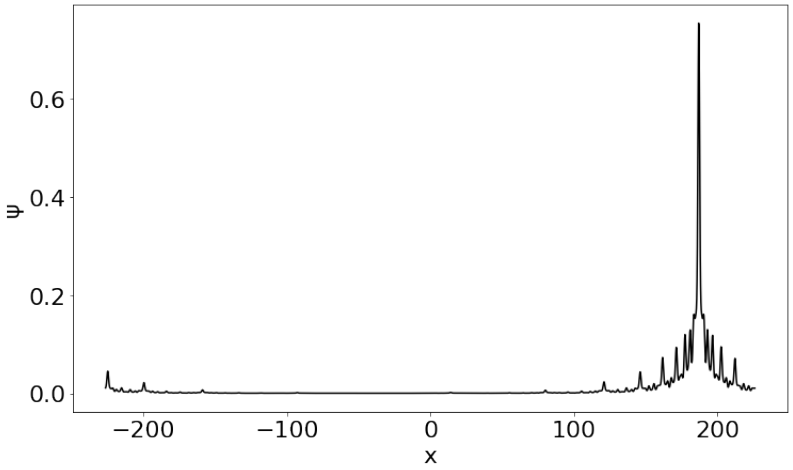

Figure 4.1: Ground state for the linear GPE for the parameters $v_1 = 0.8$; $v_2 = 0.65$; $\phi = \sqrt{2}$, $\varphi \approx \frac{233}{144}$, $\mu = -0.22606$. We can see it is asymmetrical and single humped, which will be relevant later.

4.2 Nonlinear State of the GPE

After obtaining the linear state, we must derive a way to obtain the solution to the full GPE. This means that now we are going to consider interactions among particles, and we will be working with the adimensional GPE obtained previously such that a repulsive interaction ($a > 0$) is simply represented as choosing $g = 1$ in the GPE, and an attractive interaction ($a < 0$) is translated as $g = -1$. So, the equation we are interested in solving is:

$$\mu\psi(x) = \left[-\frac{1}{2}\frac{\partial^2}{\partial x^2} + V(x) + g|\psi(x)|^2\right]\psi(x). \tag{4.7}$$

Now this is an eigenvalue problem on a nonlinear equation, which is a harder problem to solve computationally. There are many possible ways to solve this, one of which is the Newton method. This method from numerical analysis is one that on its simplest form can approximate roots of many real valued functions of a single variable $f(x)$. Supposing we want to approximate the root x^s such that $f(x^s) = 0$ all we need is an initial guess x^0 such that $f'(x^0) \neq 0$. From this we will iteratively calculate the next point, such that:

$$\begin{aligned} x^{m+1} &= x^m - \frac{f(x^m)}{f'(x^m)}, \\ x^1 &= x^0 - \frac{f(x^0)}{f'(x^0)}. \end{aligned} \tag{4.8}$$

Since we are working numerically we must settle for a predefined accuracy where instead of checking if $f(x^m) = 0$ we will check if $|f(x^m)| < \epsilon$, where ϵ is the prescribed accuracy (which can be for example 10^{-8}). This is to reduce numerical errors that come from us having finite machine accuracy.

In order to apply this method to the GPE we must adapt it to a system of equations, since we will be solving N_x equations of N_x variables, one for each point of the domain the Condensate is in. We can rewrite the recursive formula above in the following way:

$$f'(x^m) \cdot \left(x^{m+1} - x^m\right) = -f(x^m). \tag{4.9}$$

If instead of a singular variable x we now have N_x variables it is useful to define $\vec{x} = \left(x_0, x_1, ..., x_{N_x}\right)$ as the vector of variables. Since we are now looking at a multivariate function, instead of the derivative we must have the Jacobian matrix, which is defined as the matrix that contains all of its first order derivatives $J_{i,j} = \frac{\partial F_i}{\partial x_j}$. So the equation we want to solve becomes:

$$J \cdot (\vec{x}^{m+1} - \vec{x}^m) = -F(x^m). \tag{4.10}$$

Since we are working with a matrix that may be very large it is much easier to solve the linear system in order to find the increment to the vector (because that is what $x^{m+1} - x^m$ represents) than it would be to invert the Jacobian matrix. For our problem, $F(x^m)$ is simply the GPE (4.7) in its discretized version. Since this Newton method is good for finding roots of functions we must rewrite the GPE as such:

$$\left[-\frac{1}{2}\frac{\partial^2}{\partial x^2} + V(x) - \mu + g|\psi(x)|^2\right]\psi(x) = 0. \tag{4.11}$$

Now we must take into account the discretization of this equation, which will be similar to the linearized GPE from last section, and will have the following expression:

$$-\frac{1}{2\Delta x^2}\psi_{i-1} + \left(V_i - \mu + \frac{1}{\Delta x^2} + g|\psi_i|^2\right)\psi_i - \frac{1}{2\Delta x^2}\psi_{i+1} = 0. \tag{4.12}$$

Similarly to the matrix that arises from the discretization of the GPE, the Jacobian matrix is going to be similarly sparse and will be defined the following way:

$$\begin{aligned} J_{j,j} &= V_j + \frac{1}{\Delta x^2} - \mu + g\left(2|\psi_j|^2 + \psi_j^2\right), \\ J_{j,j+1} = J_{j+1,j} &= -\frac{1}{2\Delta x^2}, \\ J_{1,N_x} = J_{N_x,1} &= -\frac{1}{2\Delta x^2}. \end{aligned} \tag{4.13}$$

Differently from the linear state, the nonlinear state is not necessarily normalized to unity. With this in mind, we can now apply the Newton method to the GPE in order to find the nonlinear states. As for the single variable case we need an initial guess, which we will take as the linear state of the GPE, obtained by the method described in the previous section, and we will represent it as ψ^0. We must also choose a chemical potential, and our choice must be relatively close to the original potential of the linear state in order for us to stay in the basin of attraction of a nonlinear solution. After setting an accuracy we may iterate the algorithm until $|\psi^{m+1} - \psi^m| < \epsilon$, which we will then consider as our final answer. As an example we provide in Figure 4.2 the nonlinear state for a repulsive particle interaction ($g = 1$), for the parameters $v_1 = 0.8; v_2 = 0.65; \phi = \sqrt{2}; \varphi \approx \frac{233}{144}$ and a chemical potential $\mu = -0.2211$

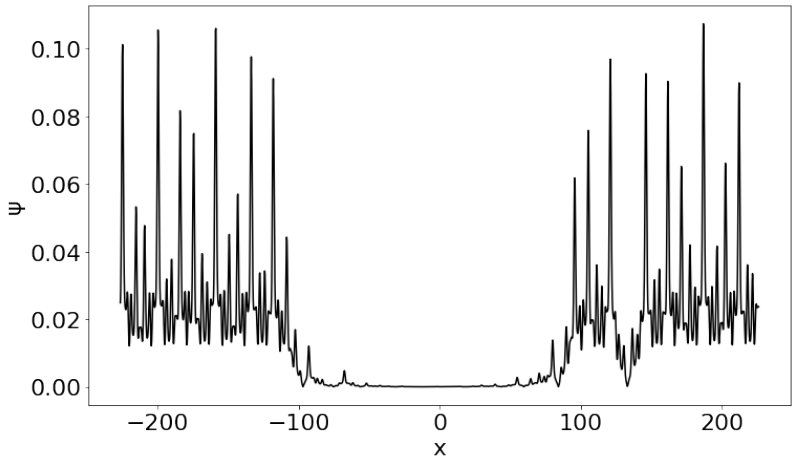

Figure 4.2: Nonlinear state of the GPE with repulsive interaction obtained by the Newton Method with the same parameters as the state from Figure 4.1 and chemical potential $\mu = -0.2211$.

4.3 Sweeping Method for GPE

As said in the previous section, in order for us to obtain the nonlinear state using a Newton method, it is necessary to "guess" the chemical potential and hope that the linear state we are using as initial guess is inside the convergence zone. As such, we can use a more systematic way that will improve our chances of finding states. This can be done with the so called sweeping method, which will make it so that instead of guessing what the chemical potential might be we set a constant increment that we are going to add at every step to our chemical potential. This way we can set for example $\Delta\mu = 10^{-3}$, which will make it so it is very likely that our Newton method will converge. The method can be described in the following way:

1. Calculate the linear ground state ψ^0 and calculate the chemical potential μ_g as the ground state chemical potential;
2. Add a predefined $\Delta\mu$ to the chemical potential;
3. Using the ground state ψ^0 as initial guess and the chemical potential $\mu^1 = \mu_g + \Delta\mu$, calculate the nonlinear state using the Newton method;
4. After obtaining the state ψ^1, repeat the process using it as initial guess and the chemical potential $\mu^2 = \mu^1 + \Delta\mu$;
5. Iterate until desired chemical potential is reached.

This method makes it so we increase our chances of finding a nonlinear state and provides us with a great amount of states, making it easier to study the properties of a BEC.

4.4 Bogoliubov-de Gennes Equations

In this section we are going to talk about one of the most important parts of this thesis, the Bogoliubov-de Gennes equations. Since we want to study the formation and propagation of matter waves in BECs it is necessary to understand how a BEC reacts to excitations around a steady state. The study of these equations is related with the previously mentioned Bogoliubov prescription, in which we consider our condensate to be an average value for the wavefunction plus some small oscillation, which we ignored when deriving the GPE. Now we will be interested in understanding these oscillations and their dynamics. These elementary

excitations have been thoroughly studied, both analytically [29, 30] and numerically [31]. This method may also be used to evaluate the linear stability of any stationary state of a BEC. In this section we are interested in showing the analytical derivation of the BdG equations, followed by the numerical methods used to solve them. Looking again at the Bogoliubov prescription $\psi = \psi^0 + \delta\psi$, we previously ignored the fluctuation term, leaving simply the expected term. Now we are going to keep this term in the GPE in order to look at the dynamics that arise from this. But we will substitute a specific ansatz for the perturbation, which takes the form:

$$\psi(x,t) = e^{-i\mu_g t}\left[\psi_g(x) + u^\epsilon(x)e^{-i\omega t} - \bar{v}^\epsilon(x)e^{i\bar{\omega}t}\right], \tag{4.14}$$

where ψ_g is the steady state of the condensate, μ_g is the chemical potential of that state and $u^\epsilon(x), v^\epsilon(x)$ are the Bogoliubov excitation amplitudes, treated as small perturbations. ω is the eigenfrequency of the perturbations, which may be complex. We will explore this further on. Now we will substitute this ansatz in the GPE and expand to first order in the perturbations, obtaining the following coupled equations:

$$\begin{aligned}\omega u^\epsilon(x) &= \left[-\frac{1}{2}\nabla^2 + V(x) + 2g|\psi_g(x)|^2 - \mu_g\right]u^\epsilon - g\psi_g^2 v^\epsilon(x),\\ -\omega v^\epsilon(x) &= \left[-\frac{1}{2}\nabla^2 + V(x) + 2g|\psi_g(x)|^2 - \mu_g\right]v^\epsilon - g\bar{\psi}_g^2 u^\epsilon(x).\end{aligned} \tag{4.15}$$

It is important to note that physically relevant Bogoliubov eigenfunctions satisfy the following normalization condition:

$$\int\left[|u^\epsilon(x)|^2 - |v^\epsilon(x)|^2\right]dx = \frac{1}{N_0}, \tag{4.16}$$

with N_0 the number of particles in the condensate. We are going to normalize the eigenfunctions:

$$u = \sqrt{N_0}u^\epsilon; v = \sqrt{N_0}v^\epsilon, \tag{4.17}$$

such that (4.16) is now normalized to 1. This normalization does not change the system (4.15), which we can identify as an eigenvalue problem. We can look at its matrix form, which is the following:

$$\begin{bmatrix} H_- + g|\psi_g|^2 & -g\psi_g^2 \\ g\bar{\psi_g}^2 & -H_- - g|\psi_g|^2 \end{bmatrix} \begin{bmatrix} u(x) \\ v(x) \end{bmatrix} = \omega \begin{bmatrix} u(x) \\ v(x) \end{bmatrix}, \tag{4.18}$$

Where the Hamiltonian operator is just the regular Hamiltonian from the GPE

$$H_- = -\frac{1}{2}\nabla^2 + V(x) + g|\psi_g|^2 - \mu_g. \tag{4.19}$$

Now that we can formulate the problem entirely using a matrix we can discretize the equation as we did previously. Using the same periodic boundary conditions as the underlying condensate and the central difference method again for the laplacian, the discretization is similar to the cases we looked at in the previous sections. The matrix is a block matrix of size $2N_x \times 2N_x$, and we can characterize each of the blocks separately, as each will be a matrix of size $N_x \times N_x$. Starting with the off-diagonal blocks, these will be diagonal matrices, with the following form:

$$b_{i,i} = g(\psi_g)_i^2, \tag{4.20}$$

And the diagonal blocks take the almost same form as the matrix from the previous sections:

$$\begin{aligned} a_{i,i} &= \frac{1}{\Delta x^2} + V_i - \mu_g + 2g(\psi_g)_i^2, \\ a_{i+1,i} &= a_{i,i+1} = -\frac{1}{2\Delta x^2}, \\ a_{1,N_x} &= a_{N_x,1} = -\frac{1}{2\Delta x^2}. \end{aligned} \tag{4.21}$$

We see that our eigenvector will be $2N_x$ in length, and as such when time comes to interpret the results we must have in mind that the first N_x elements will be the u perturbation and the rest will be the v perturbation. Now this becomes again a problem of diagonalizing the matrix and finding out the solutions. In the case of the BdG equations the eigenvectors aren't necessarily real, it is very possible that our resulting wavefunctions are complex, and the same is true for the eigenvalues, which will be relevant when we want to do linear analysis of the stability of the condensate. For that it is important to note that a property of the BdG Equations. If (ω, u, v) is a solution to the BdG Equation, then $(\bar{\omega}, \bar{u}, \bar{v})$ is a solution as well. This can be verified by taking the complex conjugates of (4.15) and solving the equations. Besides that, their eigenvalues also obey the following relation:

$$(\omega - \bar{\omega}) \int (|u(x)|^2 - |v(x)|^2) dx = 0. \tag{4.22}$$

From this equation we can see that either one of the factors is zero. If the eigenvalue ω is entirely real then $\omega - \bar{\omega} = 0$, and so we still are under the normalization we defined before where (4.16) is 1. If, on the other hand, $\omega - \bar{\omega} \neq 0$ this means two things; first that ω is complex and that $\int (|u(x)|^2 - |v(x)|^2) dx = 0$, meaning that both components of the perturbation have the same modulus.

4.4.1 Linear Stability Analysis

Now we are going to explain one the possible applications of the BdG equations and the most used in this thesis, which is linear stability analysis. As said before the eigenvalues of the BdG Equations may be complex or real, and the stability of the ground state of the condensate depends on that fact. If they are real then the state is stable, if they contain a non-zero complex part the state is unstable. This can be explained by looking at the way we introduced the perturbations to the condensate. Looking at (4.14) we see that the components u and v are multiplied by a complex exponential $e^{i\omega t}$. If the frequency ω is entirely real then this is just an oscillation, meaning that the overall modulus of the perturbation will be conserved, changing only by a phase. If, on the other hand, the frequency has a nonzero imaginary part we may represent it as $\omega = a + bi$, and the exponential will be now e^{iat-bt}. As time propagates, if $b > 0$ then this exponential will vanish, but if $b < 0$ then the exponential will increase in modulus, proving our condensate to be unstable. As we saw earlier, when ω is an eigenvalue then so is $\bar{\omega}$. This is important because as long as we have one complex value that means we will have an unstable perturbation, that will make the condensate unstable. As we move on to the dynamical evolution of the condensate this will be important, and we will explain that in the next section.

4.5 Dynamical Evolution

All the methods explained in the previous sections were used to obtain information about the ground state of the condensate. The ansatz used to obtain these states made it so time evolution just represented a global phase of the condensate. Now we want to consider time evolution, because we want to understand the evolution of the perturbations or how the

instability of the condensate evolves over time. So, instead of the previous equations now we are interested in solving the time dependent GPE:

$$i\frac{\partial}{\partial t}\psi(\vec{r},t) = \left[-\frac{1}{2}\nabla^2 + V(\vec{r}) + g|\psi(\vec{r},t)|^2\right]\psi(\vec{r},t). \tag{4.23}$$

There are many numerical methods we can use to consider this evolution. We could use for example the split step Fourier Transform or the Sine Spectral Method, but we chose to use a Crank-Nicolson semi implicit finite difference method [32]. This choice of a semi implicit method comes from the fact that if we utilized a fully implicit method it would be very computationally expensive. We can see this by writing the would-be equation. Using the central difference method for discretizing in the space domain and the forward difference method for discretizing in the time domain, with a time step $\Delta t = \frac{T}{N_T}$, T the final time we want to evolve to and N_T the number of time steps, we would need to solve the equation:

$$i\frac{\psi_j^{n+1} - \psi_j^n}{\Delta t} = -\frac{1}{4}\nabla^2\left(\psi_j^{n+1} + \psi_j^n\right) + \left[V_j^n + g(|\psi_j^n|^2 + |\psi_j^{n+1}|^2)\right](\psi_j^{n+1} + \psi_j^n). \tag{4.24}$$

As we can see, for each time step we would need to solve a nonlinear system of equations, which would be very computationally expensive. We would also need extreme numerical accuracy in order to obtain good results. Because of that we instead chose to use a Crank Nicolson semi implicit finite difference method. This name is given because we are going to mix the Crank Nicolson method, which we use for the time domain, and semi implicit because we are simplifying the system we need to solve to a linear one. This method is unconditionally stable. With that in mind, the system we now want to solve is the following:

$$i\frac{\psi_j^{n+1} - \psi_j^n}{\Delta t} = -\frac{1}{4}\left[\frac{\psi_{j-1}^n - 2\psi_j^n + \psi_{j+1}^n}{\Delta x^2} + \frac{\psi_{j-1}^{n+1} - 2\psi_j^{n+1} + \psi_{j+1}^{n+1}}{\Delta x^2}\right] + \left[V_j^n + g|\psi_j^n|^2\right]\psi_j^n, \tag{4.25}$$

which can be rewritten as follows:

$$\begin{aligned} \psi_{j-1}^{n+1} + \frac{2\left(-\Delta t + 2i\Delta x^2\right)}{\Delta t}\psi_j^{n+1} + \psi_{j+1}^{n+1} = \\ -\psi_{j-1}^n + 2\left(1 + \frac{2i\Delta x^2}{\Delta t} + 2\Delta x^2 V_j^n + 2\Delta x^2 g|\psi_j^n|^2\right)\psi_j^n - \psi_{j+1}^n. \end{aligned} \tag{4.26}$$

This can be rewritten as a matrix equation in the following manner:

$$\psi^{n+1} = Q^{-1} H^n \psi^n. \tag{4.27}$$

So now we only need to say what are the matrix elements, and then this becomes again simply a problem of solving the system. We must keep in mind that we are still using periodic boundary conditions, which will change these matrices. We see that the H^n matrix has a superscript, we can interpret this as the Hamiltonian matrix and it will evolve over time due to the nonlinear term, which obviously changes with each time step. Both the Hamiltonian and the Q matrix are square $N_x \times N_x$ matrices, and can be characterized in the following way:

$$\begin{aligned} q_{i,i} &= \frac{2\left(-\Delta t + 2i\Delta x^2\right)}{\Delta t}, \\ q_{i,i+1} &= q_{i-1,i} = 1, \\ q_{1,N_x} &= q_{N_x,1} = 1. \end{aligned} \tag{4.28}$$

And the Hamiltonian matrix:

$$\begin{aligned} h^n_{i,i} &= 2\left(1 + \frac{2i\Delta x^2}{\Delta t} + 2\Delta x^2 V^n_i + 2\Delta x^2 g|\psi^n_i|^2\right), \\ h^n_{i,i+1} &= h^n_{i-1,i} = 1, \\ h^n_{1,N_x} &= h^n_{N_x,1} = -1. \end{aligned} \tag{4.29}$$

The terms $q_{N_x,1}; q_{1,N_x}; h_{N_x,1}; h_{1,N_x}$ come from applying our familiar boundary conditions. With all this in mind we now only need to decide on an initial state ψ^0 that we will evolve. Throughout this work, since we want to see the effects of the Bogoliubov perturbations on the condensate, in general our initial state will be $\psi_0 = \psi_g + \Omega$, where ψ_g is the nonlinear ground state obtained through the sweeping method and $\Omega = u - \bar{v}$ is the perturbation wave, which we define as the subtraction of both Bogoliubov components due to the way our ansatz is defined in (4.14).

Chapter 5

Results

Now we can begin to analyze the results obtained in this work. We will start by describing the model used, followed by looking at the effects that breaking the symmetry of the potential has on the linear modes of the condensate. After looking at the nonlinear modes that bifurcate from these linear ones we want to look for a delocalized linear ground state. From this we want to obtain the delocalized nonlinear states, both attractive and repulsive, and from that apply Bogoliubov-de Gennes analysis and look for localized matter waves in the form of Bogoliubov phonons or solitons. It is our objective to find localized matter waves arising from delocalized ground states.

5.1 Model for the BEC

We are going to work with a Bose-Einstein Condensate subject to an asymmetric quasi periodic potential. The BEC is known to be described by the Gross-Pitaevskii Equation, which in this case we will consider to be one dimensional. The equation we are interested in solving is then:

$$i\frac{\partial}{\partial t}\psi(x,t) = \left[-\frac{1}{2}\nabla^2 + V(x) + g|\psi(x,t)|^2\right]\psi(x,t), \tag{5.1}$$

where $\psi(x,t)$ is the wavefunction. This equation is normalized such that an interaction constant $g = 1$ represents a repulsive particle interaction and $g = -1$ represents an attractive particle interaction. The strength of the nonlinearity is dependant on the number of atoms $\mathcal{N} = \int dx|\psi|^2$. The potential $V(x)$ is a quasi periodic potential, and in one dimension we can implement this potential by superimposing two monochromatic standing waves such that their periods are incommensurate, for example $V_1 = v_1\cos(ax)$ and $V_2 =$

$v_2 \cos(bx + \phi)$ where ϕ is an arbitrary phase added to break symmetry and $\frac{a}{b}$ is irrational. This is possible if for example we choose the periods as $p_1 = \pi$ for the first wave and $p_2 = \frac{\pi}{\varphi}$ for the second wave and φ is an irrational number. A typical choice for irrational number is the golden ratio $\frac{1+\sqrt{5}}{2}$. Presented in Figure 5.1 is a quasi periodic potential and its constituent waves for the golden ratio φ as an irrational number and a phase difference $\phi = \sqrt{2}$. In this case, for simplicity, we will consider both waves to have the same amplitude $v_1 = v_2 = v$, and the potential will have the following expression:

$$V(x) = v\cos(2x) + v\cos(2\varphi x + \phi), \tag{5.2}$$

and we can represent it graphically:

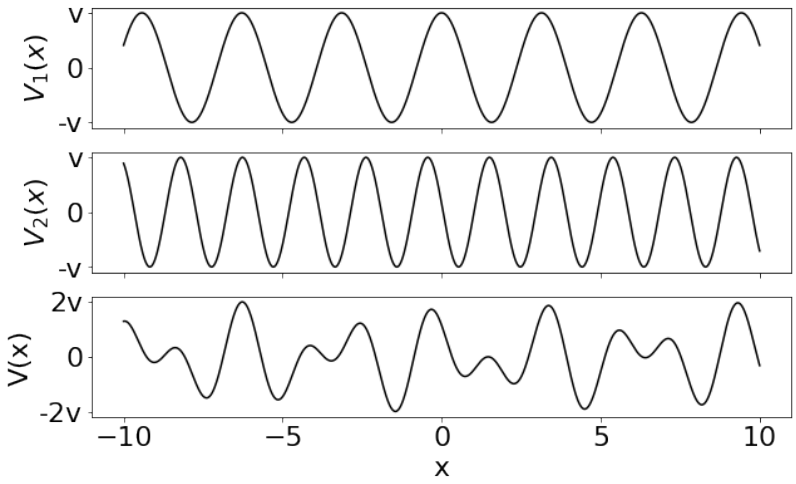

Figure 5.1: Asymmetric quasi periodic potential V and its constituent waves v_1, v_2

5.1.1 Rational Approximation

Now let us look at a technique that will be useful throughout this result section. This technique will take advantage of the fact that by definition any quasi periodic potential can be approximated by a periodic function with any desirable accuracy. Assuming that we are dealing with a large enough interval, one such way to do this in our particular case is to approximate the golden ratio φ by its Rational Approximation, given by $\varphi \approx \frac{M}{N}$, where M, N are coprime numbers. Using the golden ratio comes in handy, because obtaining a rational approximation for it is much easier than for other irrational numbers. If we use F_n to mean the n^{th} number of the Fibonacci sequence, then as $n \to \infty$ we can make good use of a property of the sequence, which is that $lim_{n\to\infty} \frac{F_{n+1}}{Fn} = \varphi$. So all we have to do is look

at two consecutive numbers of the sequence to get a good approximation. Some rational approximations are the following:

$$\varphi \approx \left[1; 2; \frac{3}{2}; \frac{5}{3}; \frac{8}{5}; \frac{13}{8}; \frac{21}{13}; \frac{34}{21}; \frac{55}{34}; \frac{89}{55}; \frac{144}{89}; \frac{233}{144}; \frac{377}{233}\right]. \tag{5.3}$$

A potential that uses any of these approximations will be periodic with a period $N\pi$. This approximation is accurate up to the vicinity of the points $N\pi$, and for that reason we will consider our condensate to exist in the interval $x \in I^N = \left[-\frac{N\pi}{2}, \frac{N\pi}{2}\right]$. In particular, let us just look at the difference between the approximation and the exact potential. Without loss of generality let's assume that $v_1 = v_2 = v$:

$$|V_N(x) - V(x)| = v|\cos\left(2\frac{M}{N}x + \phi\right) - \cos\left(2\varphi x + \phi\right)| = v|\sin(\eta)||2x\left(\frac{M}{N} - \varphi\right)|, \tag{5.4}$$

for some $\eta \in \left[-\frac{N\pi}{2}, \frac{N\pi}{2}\right]$. This equality can be obtained from the mean value theorem. If we look at any particular fixed point p then the difference will be:

$$|V_N(x) - V(x)| \leq vp|\frac{M}{N} - \varphi|, \tag{5.5}$$

which goes to 0 as we keep improving the Rational Approximation. It is also important to note that as we choose better Rational Approximations our interval will be bigger, something to keep in mind when we begin to solve the system numerically, as that will require more computational power in order to keep good accuracy. Now that we are aware of the system we will be working on and its properties it is time to look at some properties of the linear modes.

5.2 Linear Modes

In [33] great attention is given to a BEC in a symmetric quasi periodic potential. Let us now look at the effects of breaking that symmetry of the potential on the properties of the linear modes of the condensate. We will not consider interactions between particles and thus will have an interaction constant $g = 0$. First we want to look at stationary states and will use the ansatz described in (2.8). This means that the equation we want to solve is:

$$\mu\psi(x,t) = \left[-\frac{1}{2}\nabla^2 + V_N(x)\right]\psi(x,t). \tag{5.6}$$

It is necessary to specify that in our case we will be working with periodic boundary conditions, making our condensate periodic every $N\pi$ such that $\psi(-\frac{N\pi}{2}) = \psi(\frac{N\pi}{2})$.

Many of the results we are looking for in this section serve as a generalization of the work done in [33], regarding localization, memory effects and center of mass. In order for us to measure the localization of the state it is useful to define some quantities. First it is important to know how to calculate the number of atoms in the condensate, which can be done by calculating the integral:

$$\mathcal{N} = \int_{I^N} |\psi(x,t)|^2 dx, \tag{5.7}$$

where the interval I^N is the entire domain of the condensate $x \in \left[-\frac{N\pi}{2}, \frac{N\pi}{2}\right]$. Although we are defining this quantity now, for these linear states we will be working with a normalization such that $\int_{I^N} |\psi(x)|^2 dx = 1$. In order for us to measure the localization it is also important to define the Inverse Participation Ratio, in the following manner:

$$\chi = \frac{1}{\mathcal{N}^2}\int_{I^N} |\psi(x,t)|^4 dx. \tag{5.8}$$

As we can see the IPR is also dependant on the number of atoms, and the way we can measure the localization is by recognizing that the width of the state (which we will denote as ξ) is the inverse of the IPR $\xi \approx \frac{1}{\chi}$. We say that a state is localized if the width is much smaller than the size of the domain, which in this case means that $\xi \ll N\pi$.

5.2.1 Energy Spectrum and Mobility Edge

Now we can start by looking at the energy spectrum of the condensate in order to see if by breaking the symmetry there is any change regarding the memory effects and on the mobility edge observed in the symmetric case. We will look at the energy spectrum of the lowest 250 linear states of the condensate where the rational approximation used will be $\varphi \approx \frac{233}{144}$, the amplitude of the waves of the potential will be $v_1 = v_2 = v = 0.8$, the number of domain points $N_x = 2000$ (which will be maintained throughout the rest of this section) and the phase difference between constituent waves will be $\phi = 0, \sqrt{2}$. Both graphs are presented so that we can compare the two, in order to understand if the phase difference plays any part in the energy values and gaps that exist in the energy levels. We expect

mini gaps to exist regularly throughout the spectrum and larger gaps at the levels with n equal to any N present in less accurate rational approximations. In this case we are using $\varphi \approx \frac{233}{144}$, so we expect them to appear at $n = 233, 144, 89, 55, ...$ The results for these two cases can be seen in Figure 5.2.

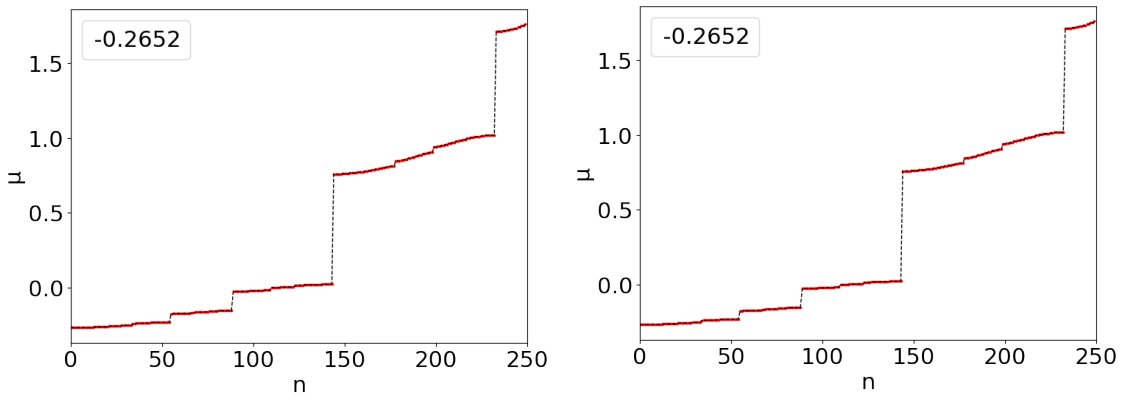

(a) Energy Spectrum for $\phi = 0$

(b) Energy Spectrum for $\phi = \sqrt{2}$

Figure 5.2: Energy spectrum for two different values of the phase difference of the waves of the potential, we can see that there is no difference between them. On both graphs the label contains the value of the energy of the energy of the ground state, which is the same on both cases.

We can see that the gaps are also located on the same levels. We clearly see that the gaps increase in size as we go to higher levels and the bigger ones appear, as expected, in the levels $n = 55, 89, 144, 233$. From this we know that the phase difference does not change the overall energy of the states, which makes physical sense. Now we want to check the mobility edge of the system, which for the symmetric case it is known that there is a transition from localized to delocalized states at the n^{th} state where $n = N$, so we expect the states of the system to go from localized at $n = 144$ to delocalized at $n = 145$. In order to check that we calculated the IPR for each one of the 250 states we obtained using the same parameters and phase difference $\phi = \sqrt{2}$, where the results can be seen in Figure 5.3.

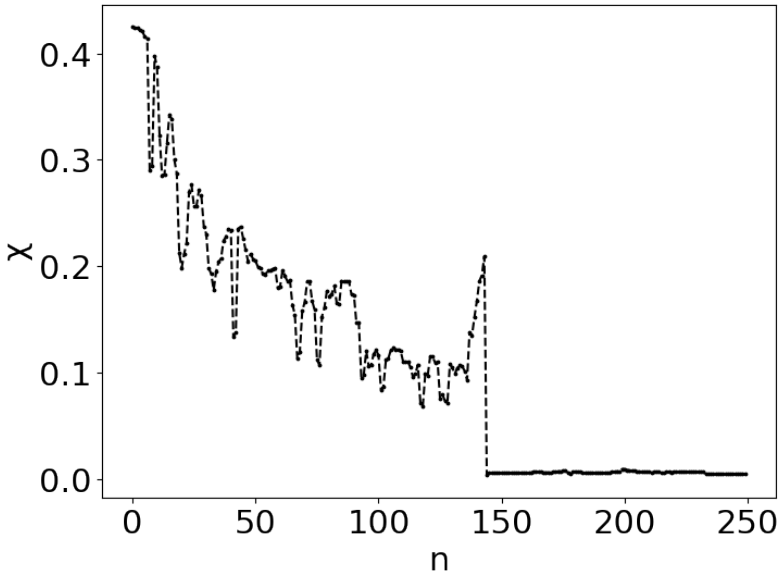

Figure 5.3: IPR for the first 250 states of the Linear Condensate with $\phi = \sqrt{2}$. A clear mobility edge is visible at the transition from the 144^{th} to the 145^{th} level.

As we can see there is a sharp drop in the IPR at the 145^{th} level, exactly as expected. It also makes sense for the ME to not be altered by the breaking of the symmetry of the potential, since it does not depend directly on it.

5.2.2 Ground State and Center of Mass

Now that we know that these properties of the system are unchanged let us look at how the ground state of the condensate may be altered. We are going to compare them for the symmetric case and for the asymmetric case.

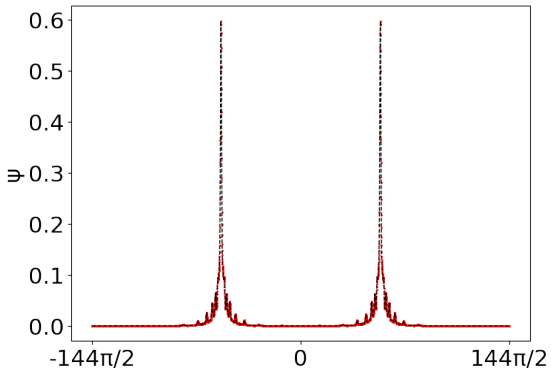

(a) Ground state of the Condensate for phase difference between waves of the potential $\phi = 0$

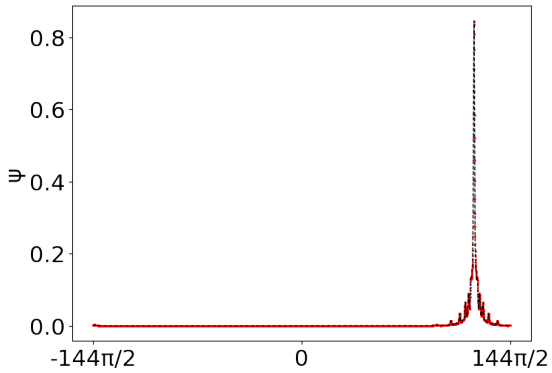

(b) Ground state of the Condensate for phase difference between waves of the potential $\phi = \sqrt{2}$

Figure 5.4: Ground state of the linearized BEC for two values of the phase difference of the waves of the potential. We see that the symmetrical case is double humped while the asymmetric is single humped.

We see that for the symmetric potential the ground state is symmetric and presents a double hump profile, whereas for the asymmetric case the state is asymmetric and single humped. Both of these states are normalized such that $\int_{I^{144}} |\psi(x)|^2 dx = 1$. It is known that the states arising from the symmetric potential are either symmetric or anti symmetric [33], which is clearly not the case for our asymmetric potential. In order to gauge the effect of breaking the symmetry on the rest of the states it may be useful to look into the center of mass of the states, dividing our interval into two smaller intervals: one defined as $I_-^N = \left[-\frac{N\pi}{2}, 0\right]$ and one defined as $I_+^N = \left[0, \frac{N\pi}{2}\right]$. Since we want to calculate the center of mass at each of the intervals we must define the two following quantities:

$$X_\pm = \frac{1}{\mathcal{N}_\pm} \int_{I_\pm^N} x|\psi(x)|^2 dx. \tag{5.9}$$

Where $\mathcal{N}_\pm = \int_{I_\pm^N} |\psi(x)|^2$, which can be seen as the number of atoms in each of the intervals of the condensate. It is known that for the symmetric potential $X_- = -X_+$, due to the fact that the states are either symmetric or anti symmetric. In our case we expect it to no longer be true, and as such we calculated the center of mass for both halves of the condensate for every state below the ME, where the results can be seen in Figure 5.5. In this figure each pair of points with the same color and the same value of μ represent one of the 144 states below the ME. One of the points will have $X < 0$ and the other will have $X > 0$.

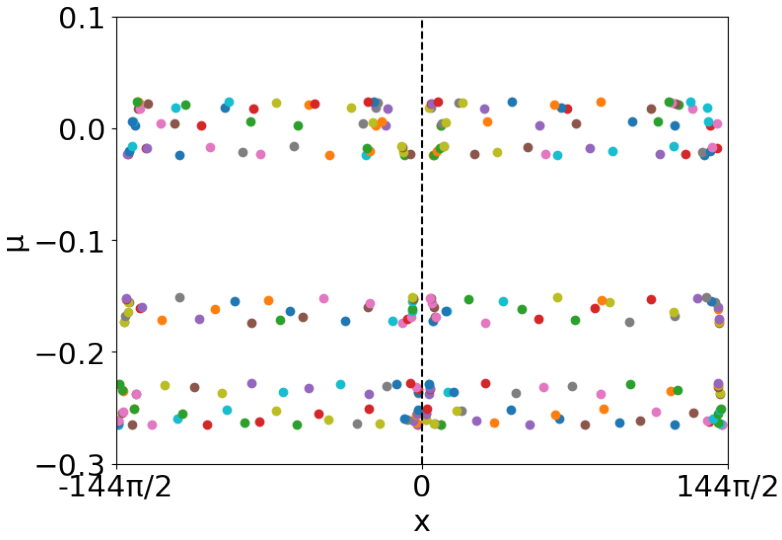

Figure 5.5: Centers of mass for the states below the ME. There is no direct relation between the centers of mass of the same state, meaning that the symmetry present in the case for the symmetric potential is gone.

From this we can clearly see that the centers of mass are no longer symmetrical, as is to be expected with a potential that no longer is symmetric as well.

5.2.3 Nonlinear Stationary States

Having looked at the properties of the linear states it is important to understand how we may obtain nonlinear states from them. In order to do this we want to take the Linear ground state and apply the sweeping method. As we account for inter particle interactions we no longer need to have the wavefunction normalized to unity, since as said before the intensity of the nonlinear term is dependant on its integral. We want to look at how the norm of the wavefunction changes as we increase the intensity of the nonlinear term and how its IPR changes as well. In order to apply the sweeping method we are going to start with the linear state for the same parameters as the previous section ($v_1 = v_2 = v = 0.8, \phi = \sqrt{2}, \varphi \approx \frac{233}{144}$), represented previously in Figure 5.4b. From this, starting at the chemical potential from the linear state μ_{linear}, we will apply the sweeping method with a variation $\Delta\mu = \pm 2.5 \cdot 10^{-3}$, where the positive variation is associated with a repulsive interaction $g = 1$ and the negative variation with an attractive interaction $g = -1$. After the states are obtained we are going to calculate the norm and IPR as said before, to see the evolution of these properties. The results can be seen in Figure 5.6.

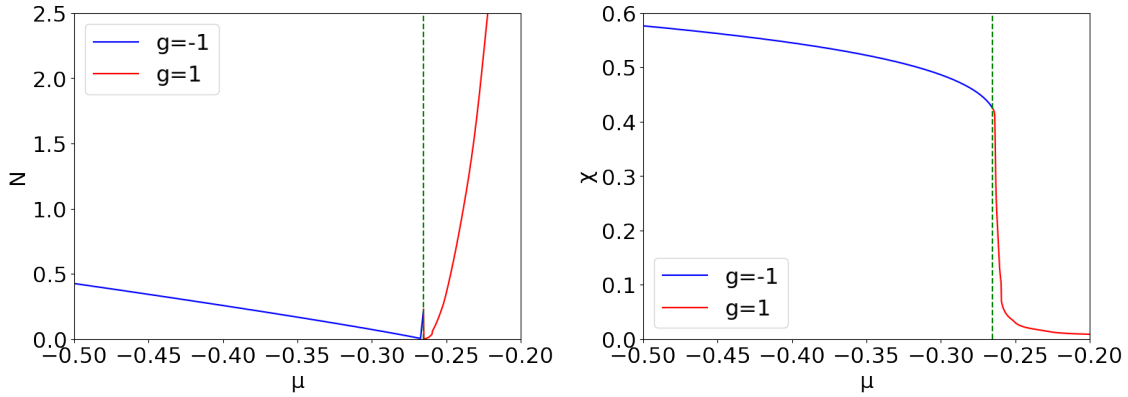

(a) Modulus of the branching states obtained via the sweeping method from the state in Figure 5.4b.

(b) IPRs of the branching states obtained via the sweeping method from the state in Figure 5.4b.

Figure 5.6: Properties of the nonlinear branching states of the condensate. We see that the way these properties change is entirely dependent on the type of particle interaction.

The green line represents $\mu = \mu_{linear}$. As expected the introduction of the nonlinearity greatly alters the properties of the condensate. They change based on the type of interaction, where we see that even if for both cases the modulus grows as we distance ourselves

from the μ_{linear}, the growth for the repulsive interaction is quicker. As for the IPR we see that it grows for the attractive interaction and it decreases close to 0 for the repulsive interaction. If we think about these trends in terms of the size of the condensate we see that for the attractive interaction the condensate shrinks as the interaction gets stronger, meaning the concentration of the atom cloud into one small area. For the repulsive interaction we have the complete opposite, since as the interaction grows in strength the condensate tends to distribute itself evenly throughout the whole domain. Now that we understand the effects of adding interaction among the particles of the Condensate, we can move on and search for a delocalized ground state, from which we can obtain localized matter waves.

5.3 Delocalized Ground State

In the previous sections, as we calculated the linear states of the condensate, we saw that the parameters used for the potential made it so the stationary state was localized. At this point we have understood the effects of breaking the symmetry of the potential, so we can proceed in our task of finding localized matter waves from delocalized ground states. In this section we are no longer going to consider the constituent waves of our potential to have the same amplitude, breaking the balance of the potential. Without loss of generality we are going to assume that $v_1 > v_2$, and starting from the previous point of balance $v_1 = v_2 = 0.8$ we are going to reduce the amplitude of the second wave, calculate the ground state and its IPR in order to evaluate how the size of the condensate changes when we reduce the amplitude of one of the constituent waves of the potential. We do this in order to evaluate whether there is a mobility edge for the strength of the potential or not. After reducing the amplitude of the second wave to zero we repeat this process for a lower value of v_1 in order to cover a wider range of potentials. The results obtained can be seen in Figure 5.7. Each of the differently colored lines represent a different value of the amplitude of the wave v_1.

We also present the graph for the size of the condensate, since it is easier to read and evaluate trends. We clearly notice the existence of an ME at $v_2 \approx 0.6$ for the amplitude $v_1 = 0.8$, and we see that the ground state is delocalized for every value of $v_2 < v_1$ when $v_1 < 0.8$. These results tell us what amplitudes to use in order to obtain the delocalized ground state.

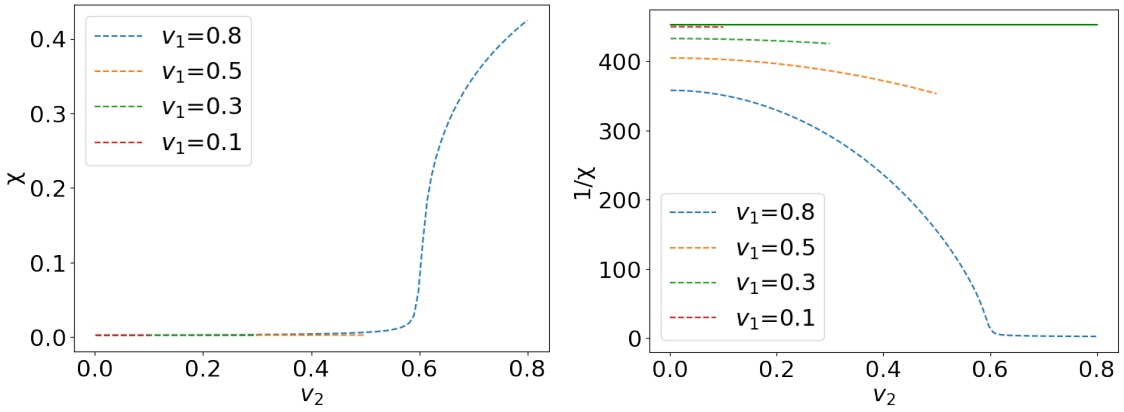

(a) IPR of the ground state for varying amplitude of the v_2 wave of the potential.

(b) Size of the ground state for varying amplitude of the v_2 wave of the potential.

Figure 5.7: IPR and size of the condensate as a function of the amplitude v_2. A mobility edge for this property can be seen at $v_2 \approx 0.6$ for $v_1 = 0.8$. The green line indicates the size of the condensate $\frac{1}{\chi} = 144\pi$

5.4 Nonlinear States

Now that we know a way to obtain a linear ground state that is delocalized we can begin to obtain the nonlinear states that branch out from them, as this process will be fundamental in our search for localized matter waves. We want to understand the effect of the particle interaction on the state. For the repulsive interaction it is expected that the state remains delocalized, whereas for the attractive interaction we must take into consideration that as we increase the strength of the interaction the state tends to localize. In this section we are going to obtain these states, on which we will do Bogoliubov-de Gennes analysis on the next section.

5.4.1 Attractive Interaction

Let's start by obtaining the states with an attractive particle interaction. As observed in Figure 5.6b, this type of interaction tends to localize the state, and thus we will want to use a combination of amplitudes of the potential that can guarantee that our initial state is delocalized. We are going to look at that initial linear state and obtain the nonlinear states branching from it. After that we will calculate the IPRs of these nonlinear states and observe the evolution of this property. For this whole section we are going to keep using the previously used RA ($\varphi \approx \frac{233}{144}$) and phase difference ($\phi = \sqrt{2}$). Starting off with the parameters $v_1 = 0.8; v_2 = 0.1$, the linear state is represented in Figure 5.8.

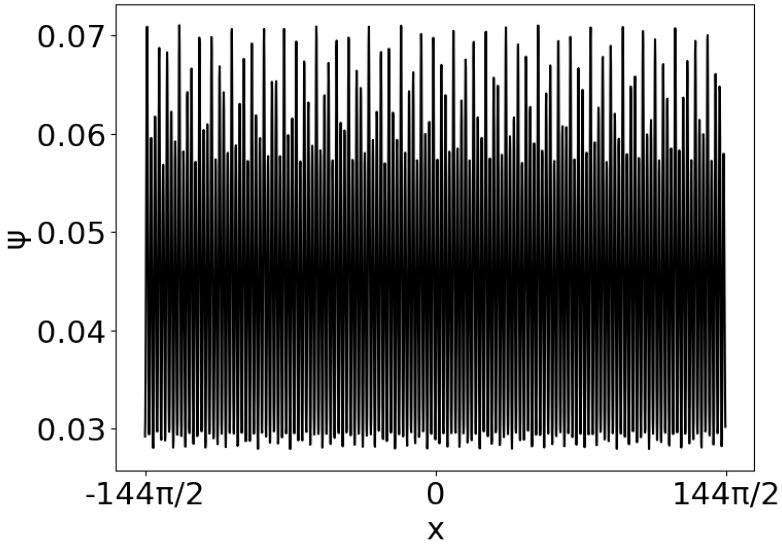

Figure 5.8: Linear ground state for $\varphi \approx \frac{233}{144}, \phi = \sqrt{2}$ and $v_1 = 0.8; v_2 = 0.1$. We can see it is delocalized, indicating that the amplitudes of the waves of the potential are adequate.

From Figure 5.8 it is simple to see that the state is delocalized. We will now use the sweeping method considering an attractive particle interaction ($g = -1$) and a step size of $\Delta\mu = -10^{-6}$. Due to convergence reasons we must use this small step, the only difference being that we will need to use more steps in order to reach a nonlinearity with a relevant effect. With that in mind we calculated 100000 nonlinear states. The evolution of the IPR as we decrease the chemical potential can be seen in Figure 5.9.

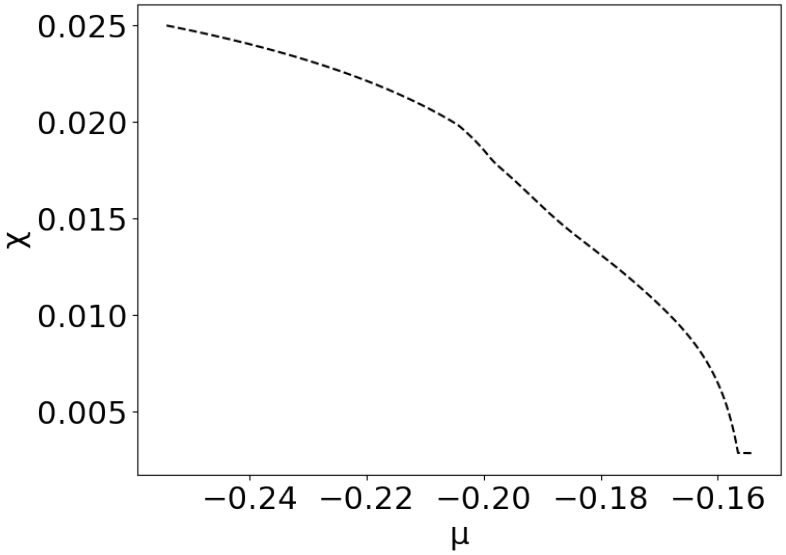

Figure 5.9: IPR of the nonlinear states branching from Figure 5.8. The trend from Figure 5.6b is reproduced, with the IPR increasing as the chemical potential decreases.

We see that as the chemical potential decreases the IPR steadily increases, indicating

a reduction of the size of the condensate. This evolution makes sense, as the attractive interaction begins to dominate the energy of the condensate.

It may also be useful to repeat this process for different values of the potential, since we can't make any judgement a priori about the stability of the states calculated above. We will, then, repeat this process for the values $v_1 = 0.8; v_2 = 0.3$. The linear state can be seen in Figure 5.10.

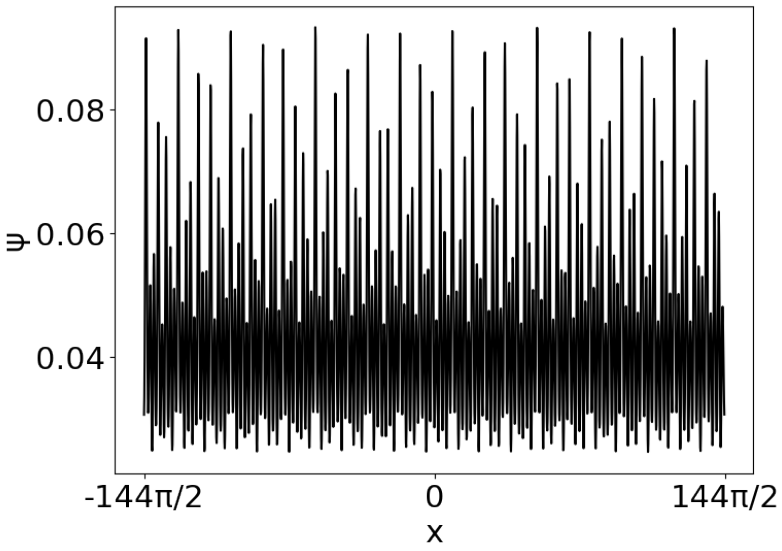

Figure 5.10: Linear ground state for the parameters $\varphi \approx \frac{233}{144}$, $v_1 = 0.8; v_2 = 0.3$ and $\phi = \sqrt{2}$. As was intended the state obtained is delocalized.

We see that this state is also delocalized, but in this case the condensate has slightly less peaks and they have a bigger modulus. Using again the same sweeping method, this time we calculated 150000 states with a step size $\Delta\mu = -5 \cdot 10^{-6}$. The results for the evolution of the IPR can be seen in Figure 5.11.

For these parameters the IPR follows the same trend as with the previous ones, having simply different values. As the chemical potential decreases it steadily grows, showing again that the nonlinear states reduce in size as the strength of the interaction grows.

5.4.2 Repulsive Interaction

Now we are going repeat this same process for a repulsive particle interaction ($g = 1$). In this case, since adding the particle interaction makes it so our state grows wider it might be more prudent to work with potential values around the mobility edge. Intuitively we may also think that as the ground state grows wider it is less likely that the oscillations around it are localized. Let's start then by calculating the Linear ground state for the

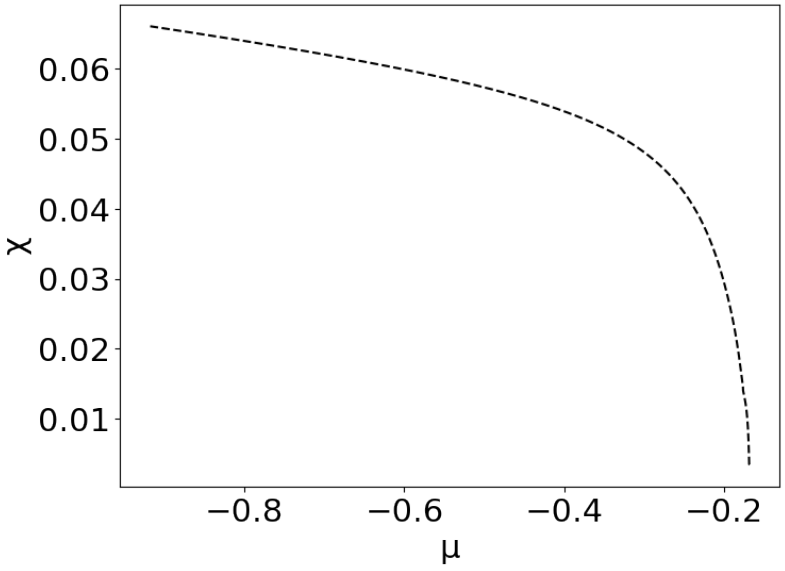

Figure 5.11: IPR of the nonlinear states branching from Figure 5.10. Again the trend from Figure 5.6b is reproduced.

potential amplitudes $v_1 = 0.8; v_2 = 0.55$. The ground state obtained is presented in Figure 5.12.

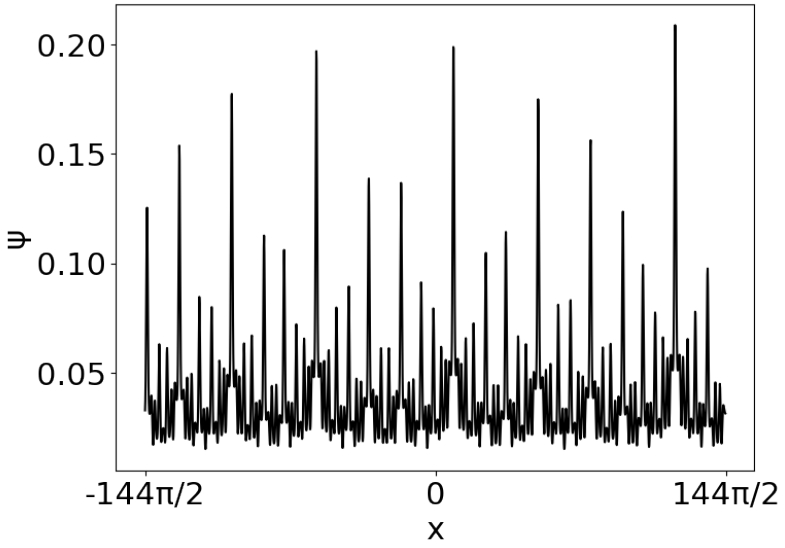

Figure 5.12: Linear ground state for the same RA and phase difference as the attractive case and potential amplitudes $v_1 = 0.8$, $v_2 = 0.55$.

We see that the state is delocalized. From this let us again apply the sweeping method, this time with a step $\Delta\mu = 5 \cdot 10^{-5}$. For this step size we calculated again 10000 states, and the evolution of the IPR with respect to the chemical potential is presented on Figure 5.13.

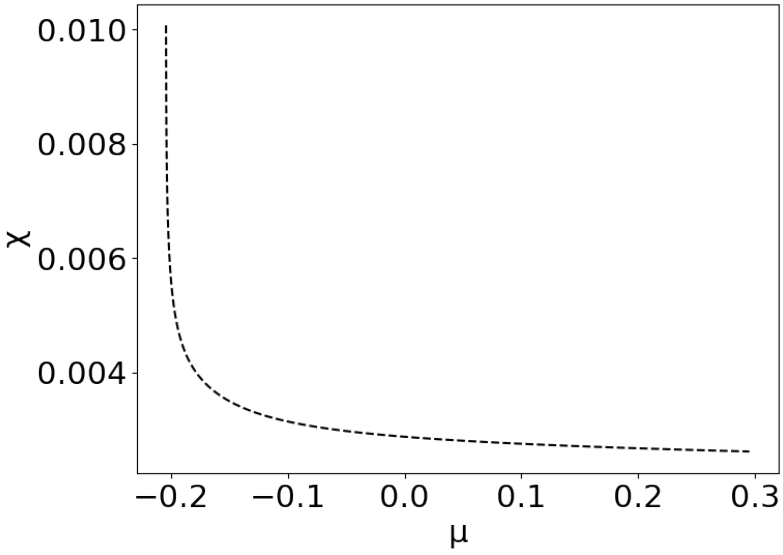

Figure 5.13: IPR of the nonlinear states branching from Figure 5.12. The trend observed in Figure 5.6b is once again reproduced, as the IPR approaches 0 as the chemical potential increases.

We see that the IPR continually decreases, signifying the growth of the states as the nonlinearity gets stronger. As before we may also want to look at the states arising from slightly different conditions, and this time we may want to look at a value of the potential slightly above the mobility edge, since we expect the state to become delocalized anyway by adding the interaction. Let's do this process again starting now with a potential $v_2 = 0.65$. The linear ground state is presented in Figure 5.14.

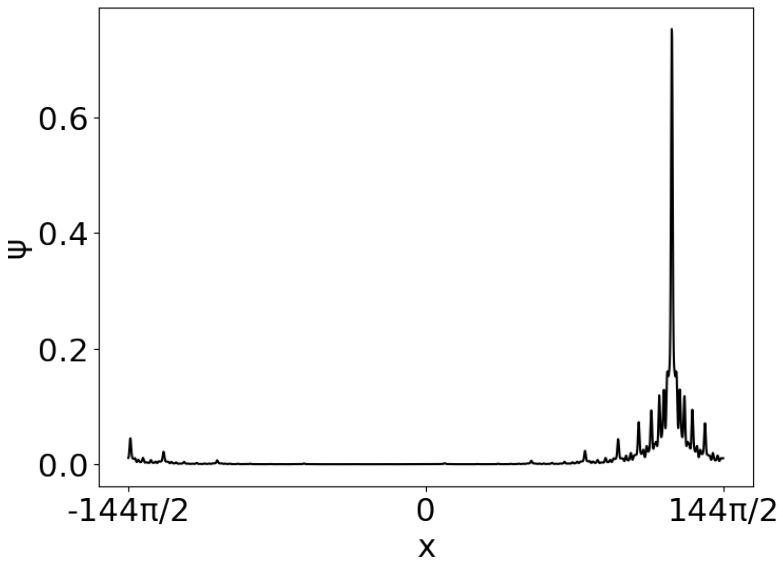

Figure 5.14: Linear ground state for the same RA and phase difference as the attractive case and potential amplitudes $v_1 = 0.8$, $v_2 = 0.65$.

As expected this state is still localized, due to the strength of the potential. Let's now add the repulsive interaction by the sweeping method, and this time we want to guarantee that the state becomes delocalized, so let's use a bigger step $\Delta\mu = 10 \cdot 10^{-4}$ and calculate 10000 states. Looking at the trend for the IPR we will obtain the Figure 5.15

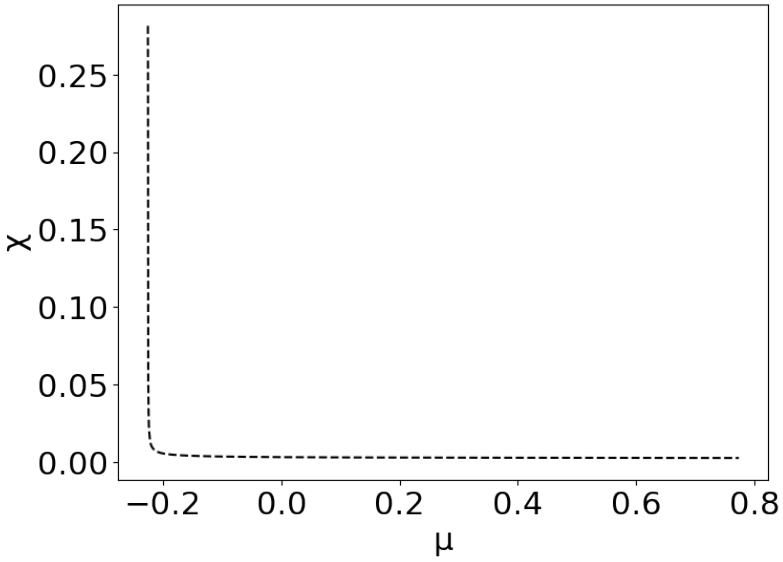

Figure 5.15: IPR of the nonlinear states branching from Figure 5.14. Once again we observe the expected trend, as the IPR decreases with the growth of the chemical potential.

We see that near the bottom limit of the chemical potential the value of the IPR is big, signifying the localized state. But as the potential increases we see that it drops to near 0, meaning that the nonlinear states become indeed delocalized.

5.5 Bogoliubov-de Gennes Analysis

Now that we have obtained the relevant nonlinear states we can start our last step, which is to try to obtain localized matter waves arising from delocalized ground states. In order to do this we are going to do stability analysis using the Bogoliubov-de Gennes analysis, which was explained in depth in the previous chapter. For this part we are going to perform the stability analysis on every nonlinear state calculated in the previous section. This will aide us in the search for the two types of matter waves we are interested. As said in the previous section, if the stability analysis of a state determines it is stable we can look for Bogoliubov phonons. In order to do this we are going to obtain the biggest value of the imaginary part of the eigenvalues calculated on the LSA. If the state is stable that value is going to be 0, if it is unstable it will be some nonzero value. We do this in order to see

if there is a sharp transition between stable and unstable nonlinear states and where it is located (if there is one), if the instability grows the further we go away from the initial Linear chemical potential or if it remains stable for every value of the chemical potential. After this has been done we can follow up and depending if we find stable or unstable states look at the respective eigenfunctions, to see if they are localized of not.

5.5.1 Attractive Interaction

As in the previous section we are going to start off with the states obtained by adding an attractive particle interaction, specifically the ones obtained from Figure 5.8 ($v_1 = 0.8; v_2 = 0.1$). The graph that represents the evolution of the largest imaginary eigenvalue as a function of the chemical potential is presented in Figure 5.16.

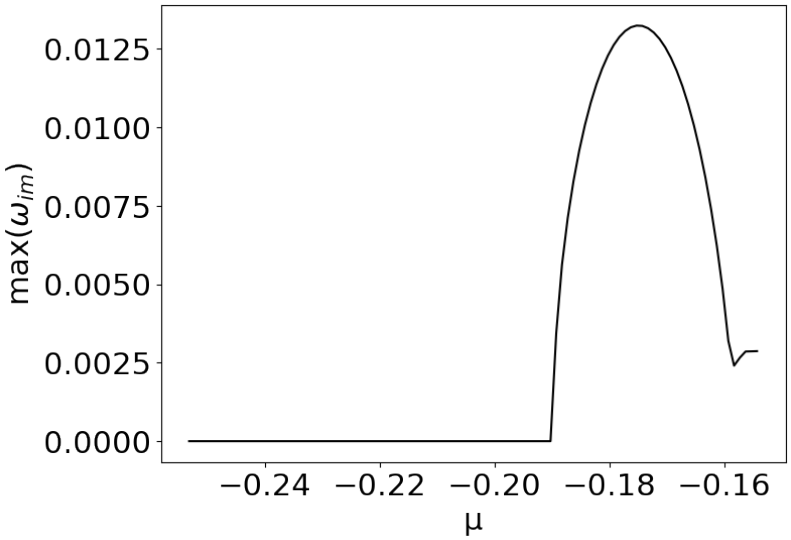

Figure 5.16: Largest imaginary eigenstate of the BdG perturbations of the states from Figure 5.9 (potential amplitudes $v_1 = 0.8; v_2 = 0.1$). A transition between stable and unstable states can be seen at around $\mu \approx -0.19$.

In order to look at this graph the correct way we must keep in mind that the states were obtained by reducing the chemical potential, so we must look at these points in the descending order of the potential. We see that there is a transition from unstable to stable at around $\mu \approx -0.19$. This transition may be explained by the fact that at that value of the potential the energy from the attractive interaction may become dominant over the energy from the potential. This means that one of these stable states is probably a suitable candidate for us to look for a localized phonon. The fact that its energy is far away from the linear energy also indicates strong nonlinearity. We can continue by looking at the other family of states obtained for attractive particle interaction, the ones obtained

from Figure 5.10 ($v_1 = 0.8; v_2 = 0.3$). Repeating the process of calculation of the largest imaginary eigenvalue as a function of the chemical potential we will obtain Figure 5.17.

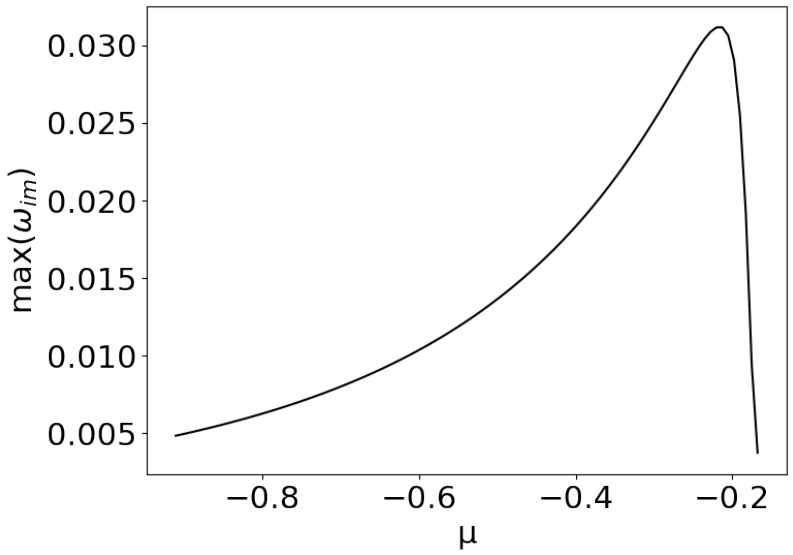

Figure 5.17: Largest imaginary eigenstate of the BdG perturbations of the states from Figure 5.11 (potential amplitudes $v_1 = 0.8; v_2 = 0.3$). Contrary to the previous image there is no transition in the stability of states, but the largest imaginary eigenvalue decreases as chemical potential decreases.

For this combination of potential amplitudes we see a different behaviour from the condensate. The states start off as unstable and the maximum imaginary part of the eigenvalues reaches a peak at around $\mu \approx -0.25$, and after that peak the maximum value tends asymptotically to zero. This means that in order to reach a stable state we would need to calculate even more branching states, but with these we can see that for the considered energy range there is no transition from unstable to stable. This suggests that these states might be suitable in our search for a localized soliton.

5.5.2 Repulsive Interaction

Now we are going to repeat this process for the states obtained by adding a repulsive particle interaction. We will be starting off by analyzing the states branching from Figure 5.12 ($v_1 = 0.8; v_2 = 0.55$). Now this graph may be analyzed by following the ascending order of the potential as usual. The results obtained can be seen in the Figure 5.18.

We see now that there is no real trend among the results obtained this time. This may be explained by the fact that we started our process with a Linear state obtained for a value of the potential that is very close to the ME, and looking back at Figure 5.7a we see that it is right on the transition from localized to delocalized, which may explain the not so well

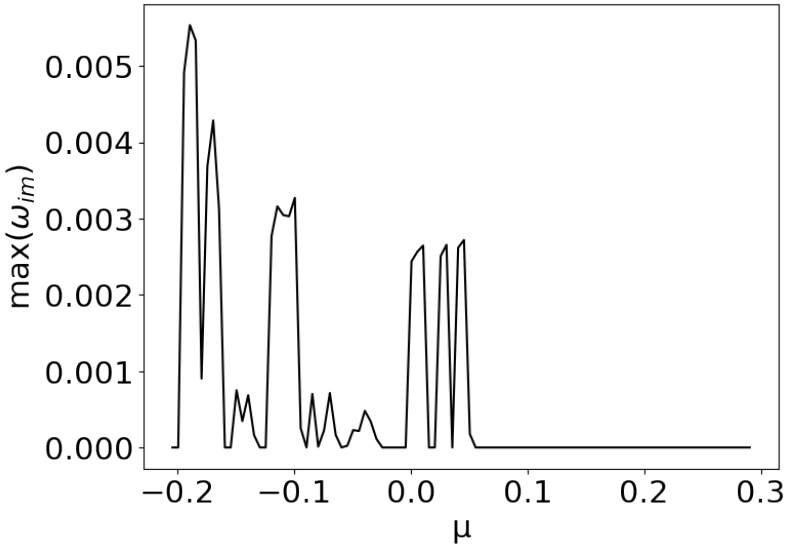

Figure 5.18: Largest imaginary eigenstate of the BdG perturbations of the states from Figure 5.13 (potential amplitudes $v_1 = 0.8; v_2 = 0.55$). No clear tendency can be observed among these states. This may be due to us being near the mobility edge for the amplitude v_2.

defined stability of the state. We see that at around $\mu \approx 0.05$ the states become all stable, where this equilibrium might be due to the repulsive interaction becoming dominant over the potential, keeping the particles in place. In spite of this dynamic these states may very well be useful to us in finding a localized phonon. This is due to the fact that even states with a chemical potential close to the chemical potential of the linear state present a strong nonlinearity, and we can make use of the stable ones in that vicinity to look for the intended phonons. To conclude we still need to obtain this same graph for the final nonlinear states we calculated previously, the ones branching from Figure 5.14 ($v_1 = 0.8; v_2 = 0.65$). The results obtained are presented in Figure 5.19.

We see that similarly to the previous graph there is no well defined trend, but like in our previous case we see that although there is an oscillation between stable and unstable states, from $\mu \approx 0.05$ onwards the states are almost all stable apart from some small fluctuations. This transition may come again from the interaction energy overpowering the energy coming from the potential. Now these states may be useful to obtain a localized soliton, since even near the linear chemical potential they are unstable. For these last two sets of nonlinear states we are going to look more at states with a chemical potential near the Linear one, and this is due to the fact that these states have a slightly bigger IPR than their more energetic counterparts, which will probably aide in finding localized excitations.

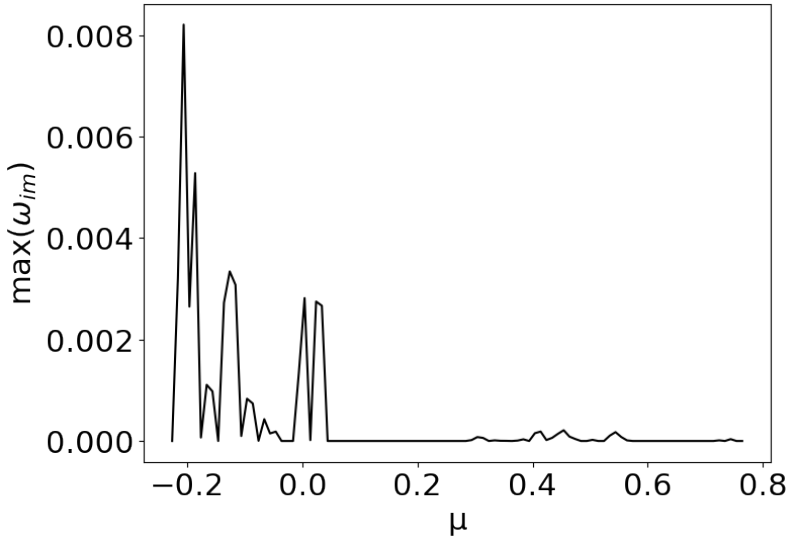

Figure 5.19: Largest imaginary eigenstate of the BdG perturbations of the states from Figure 5.15 (potential amplitudes $v_1 = 0.8; v_2 = 0.65$). Similar to the previous Figure there is no real trend regarding the stability of the states.

5.6 Localized Excitations

Now that we have an idea of what states we should look at in order to find our intended localized excitations we can finally begin this process. We will first look at states with an attractive particle interaction, followed by the repulsive interaction. In order to find our Bogoliubov Phonon we are going to take a nonlinear state previously deemed to be stable and calculate the IPR of the Bogoliubov excitations, defined as $\Omega = u - \bar{v}$ as said in the previous Chapter. If there is by chance an excitation whose IPR is big enough to correspond to a localized state then we have found our intended perturbation. For the soliton our process is going to be slightly different. We are still going to calculate the IPR of the Bogoliubov excitations but since we are later going to be interested in the time evolution of the condensate we have no choice but to look only at the excitation associated to the largest imaginary eigenvalue, since this is going to be the one that dominates the time evolution. Again, if when we look at this excitation it has an IPR large enough for us to consider it localized then all we need to do is calculate the time evolution of the condensate.

5.6.1 Attractive Interaction

Let's start by looking for our matter waves on Condensates with Attractive Particle Interaction.

5.6.1.1 Bogoliubov Phonon

Looking first for the Bogoliubov phonon, we need to find a delocalized stable nonlinear state. Like we said in the previous section a good candidate might be found among the states analyzed in Figure 5.16. Let's pick the nonlinear state with chemical potential $\mu = -0.2042$, which by looking at Figure 5.16 tells us that it is located in the stable zone. The state is presented in Figure 5.20.

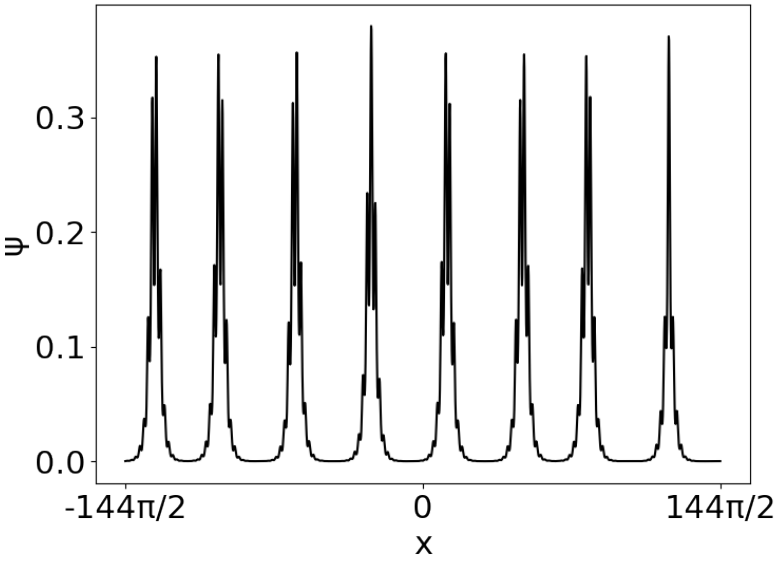

Figure 5.20: Nonlinear state for an Attractive particle interaction, amplitudes $v_1 = 0.8; v_2 = 0.1$ and chemical potential $\mu = -0.2042$ calculated in Figure 5.9. The state is delocalized just as intended.

We see that the state is delocalized. Now let us calculate the Bogoliubov-de Gennes spectrum just for this state in order to confirm its stability. We obtain the following spectrum, represented in the complex plane in Figure 5.21.

Looking at this spectrum we can see that the eigenvalues are symmetrical around the origin, and we also see that the eigenvalues of the excitations are all real, confirming that this is indeed a stable state. All that is left is for us to look at the IPRs of these perturbations in order to see if there is after all a localized one. Calculating the IPR for the states we can represent them as a function of the real part of the eigenvalue, and we are going to obtain Figure 5.22.

We see that there are indeed excitations whose IPR is large enough for it to be localized. They are all located around the eigenvalues close to 0. It is important to also note that the IPR of these eigenstates is symmetric around the origin. Let's look at the excitation with the largest IPR, which is going to be the eigenstate from Figure 5.23.

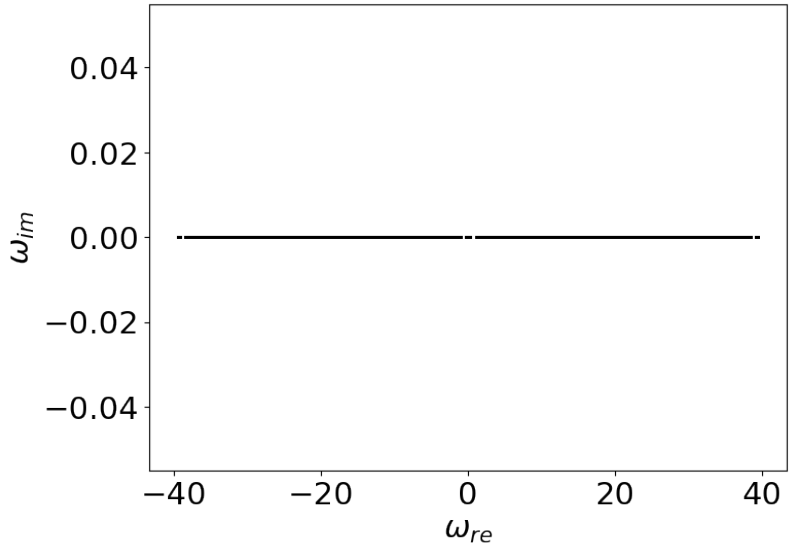

Figure 5.21: Spectrum of the Bogoliubov-de Gennes excitations for Figure 5.20. The fact that every eigenvalue is purely real indicates the state is stable.

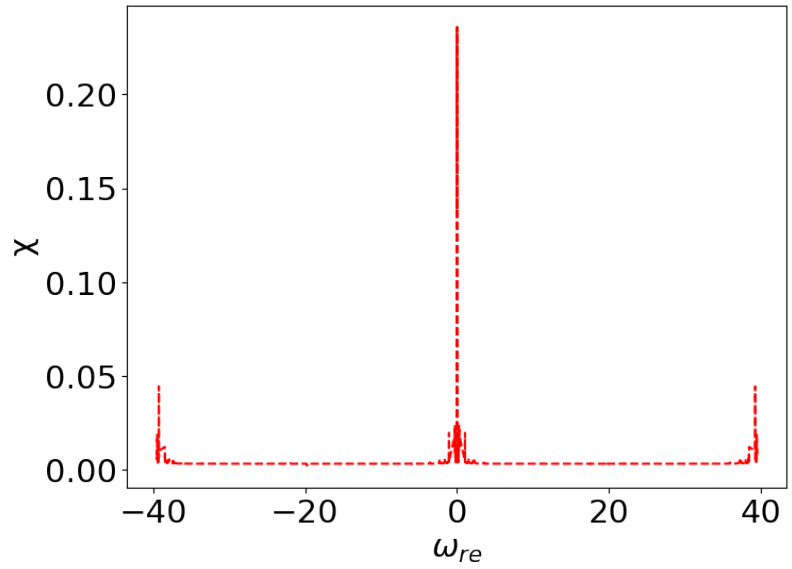

Figure 5.22: IPR of the Bogoliubov-de Gennes excitations. A clear peak is seen on the origin, indicating where to look for our intended Bogoliubov phonon.

We see that the perturbation is localized, meaning that we have found a Bogoliubov phonon as intended. Also curious is the fact that the perturbation is similar to one of the peaks of the perturbed nonlinear state.

5.6.1.2 Soliton

Let's now look for a localized perturbation arising from an unstable delocalized state. On our previous section we deemed that one of the states calculated in Figure 5.17 would be a

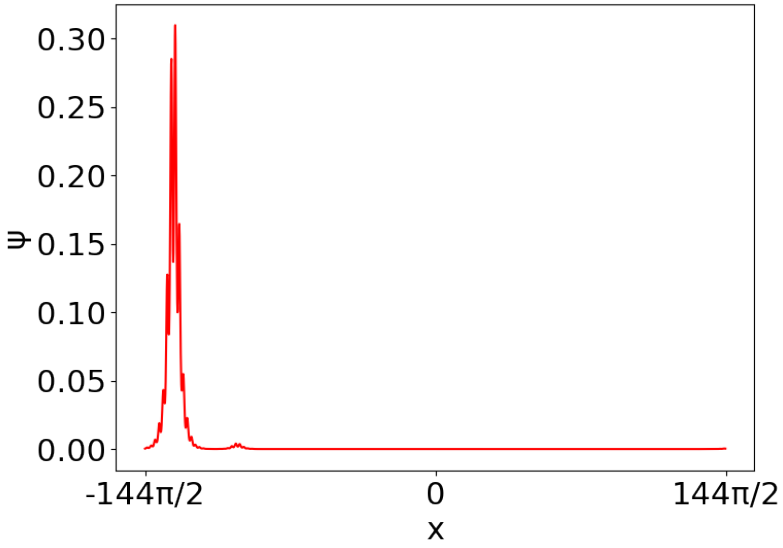

Figure 5.23: Localized perturbation for the stable state from Figure 5.20

good candidate, since we saw that most states were unstable. Let's pick again a nonlinear state we think will be suitable, for example the one with chemical potential $\mu = -0.1927$. The state is presented in Figure 5.24.

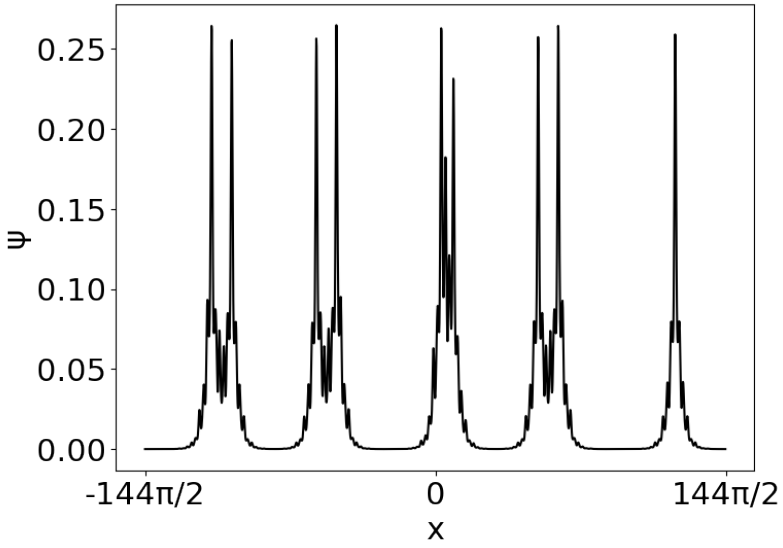

Figure 5.24: Nonlinear state for an Attractive particle interaction, amplitudes $v_1 = 0.8; v_2 = 0.3$ and chemical potential $\mu = -0.1927$ calculated in Figure 5.11. We can see that it is delocalized.

We see once again that as expected the state is delocalized and has a similar profile to the one from the previous subsection. Now once again we must calculate the Bogoliubov-de Gennes spectrum in order to see if the state is indeed unstable. After calculating the spectrum we can represent it again in the complex plane in Figure 5.25.

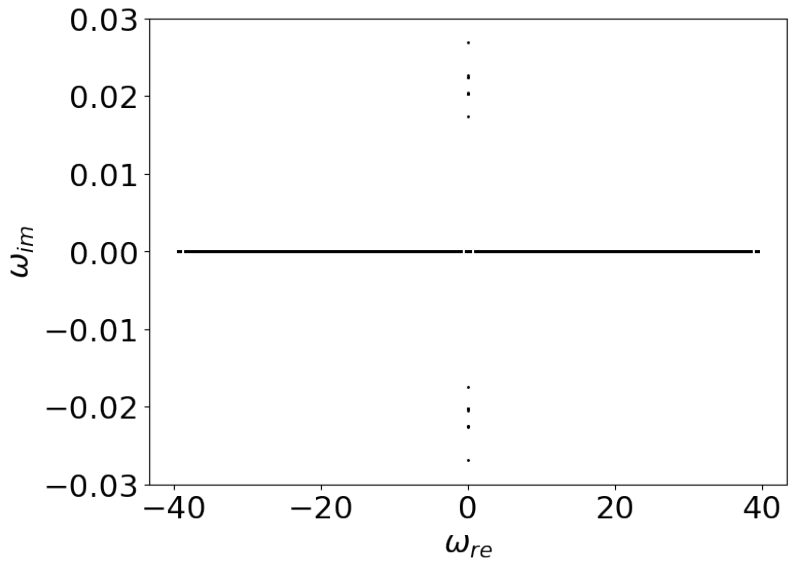

Figure 5.25: Spectrum of the Bogoliubov-de Gennes excitations for Figure 5.24. Contrary to the previous BdG spectrum we can now observe imaginary values, indicating that the state from Figure 5.24 is unstable.

From this spectrum we can confirm that it possesses the expected analytical properties, like the fact that if ω is an eigenvalue then $\bar{\omega}$ is an eigenvalue as well. We clearly see that there are states with a nonzero complex part, indicating that the underlying nonlinear state is unstable. Now we must confirm that the excitation associated with the eigenvalue with the largest imaginary part ($\omega = 0.02689i$) is localized. We can do that by calculating just the IPR of that state and determining whether it is localized or not. The state is represented in Figure 5.26.

The IPR of this state is calculated to be $\chi = 5.6322$ and we can see that it is localized. Once again we have found the state we were looking for. We have now found the two types of perturbations we were looking for, meaning that we can move on to states with a repulsive particle interaction and look for these perturbations there as well

5.6.2 Repulsive Interaction

Now we want to repeat this process but for a Repulsive Particle interaction. Here we face the problem that as the interaction strength grows the nonlinear states tend to delocalize, and even though we are interested in delocalized nonlinear states we must choose them from a point of relative equilibrium between the Repulsive interaction and the kinetic and potential energies of the particle. Let's begin again by finding a Bogoliubov phonon from a stable nonlinear state.

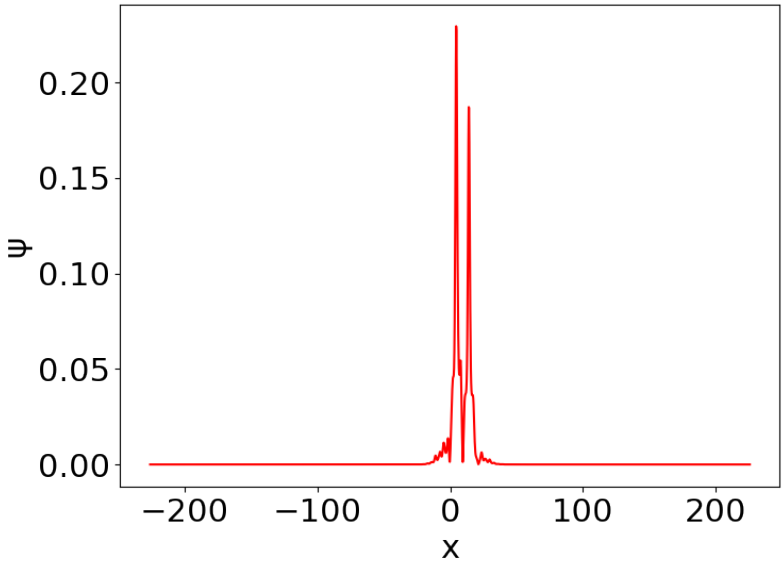

Figure 5.26: Localized perturbation associated with the largest imaginary eigenvalue of the spectrum 5.25 for the state from Figure 5.24.

5.6.2.1 Bogoliubov Phonon

We can begin again by looking for a stable nonlinear state, and looking back at Figure 5.18 it tells us that we can look here for a stable nonlinear state. Looking for example at the state with a chemical potential $\mu = -0.2042$ we can see it in Figure 5.27.

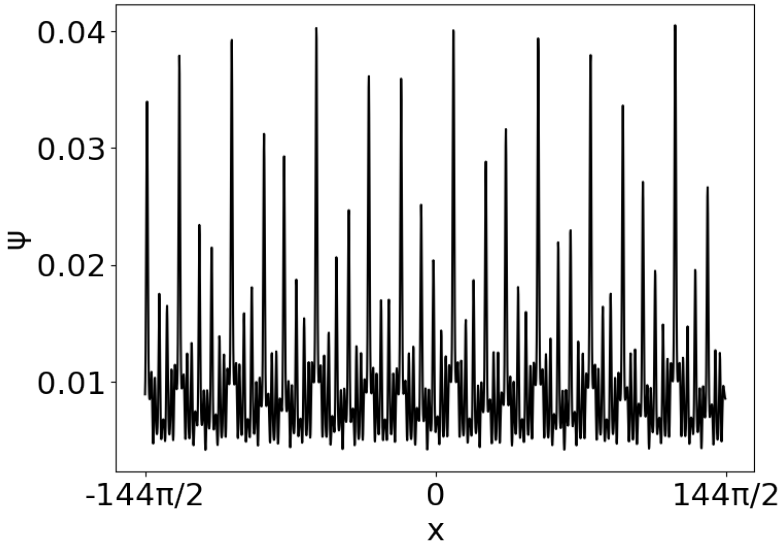

Figure 5.27: Nonlinear state for a Repulsive particle interaction, amplitudes $v_1 = 0.8; v_2 = 0.55$ and chemical potential $\mu = -0.2042$ calculated in Figure 5.13.

Again this state is delocalized, signaling us that we can go ahead and determine its stability by calculating the Bogoliubov-de Gennes spectrum. Representing the spectrum in the complex plane we are going to obtain the Figure 5.28.

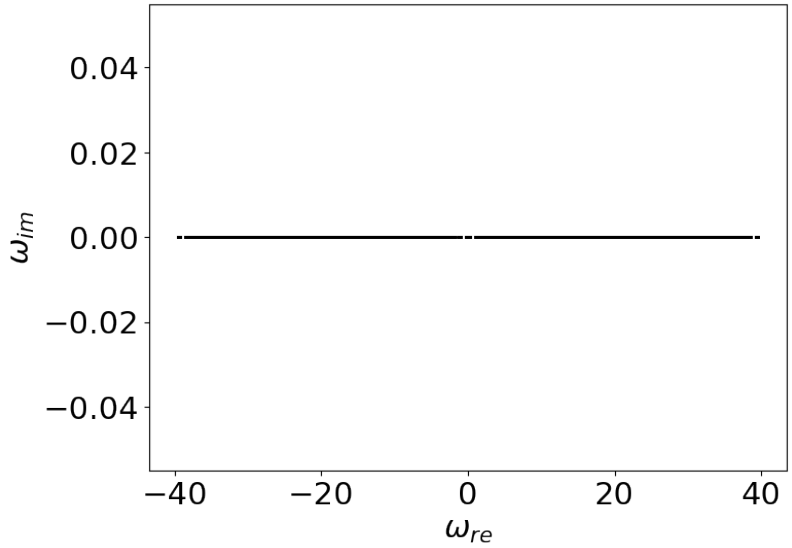

Figure 5.28: Spectrum of the Bogoliubov-de Gennes excitations for Figure 5.27. We see that it its eigenvalues are entirely real, indicating the state from Figure 5.27 is stable.

We see in this case that the spectrum contains only real values, meaning that the chosen nonlinear state is indeed stable. All that is left now is to again calculate the IPRs of these perturbations in order to conclude if there is a localized perturbation. Calculating these values and representing them as a function of the real part of the eigenvalues we are going to obtain Figure 5.29.

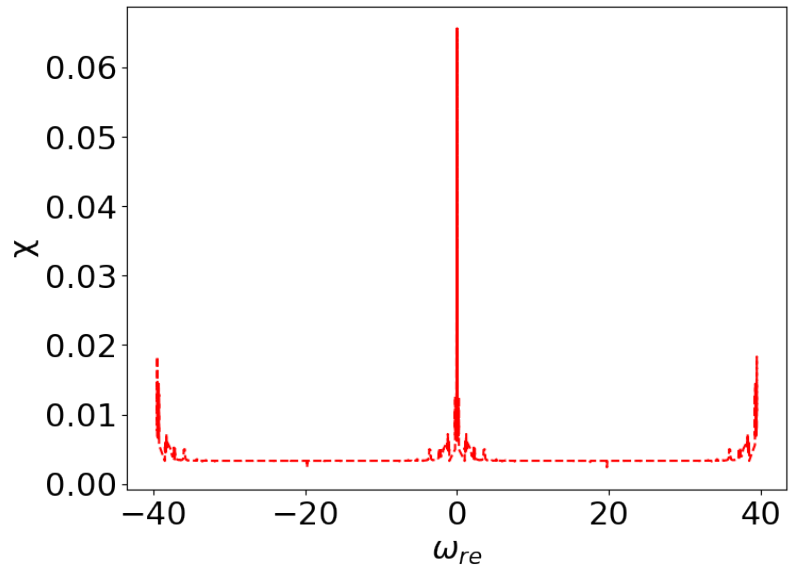

Figure 5.29: IPR of the Bogoliubov-de Gennes excitations. Once again there is a noticeable peak on the origin, indicating where to look for localized excitations.

We see again that by looking at the IPRs there are excitations with an eigenvalue close to 0 that are localized, meaning that once more we were able to find the intended

excitation. Let's look again at the excitation associated to the biggest IPR, and it has the following form presented in Figure 5.30.

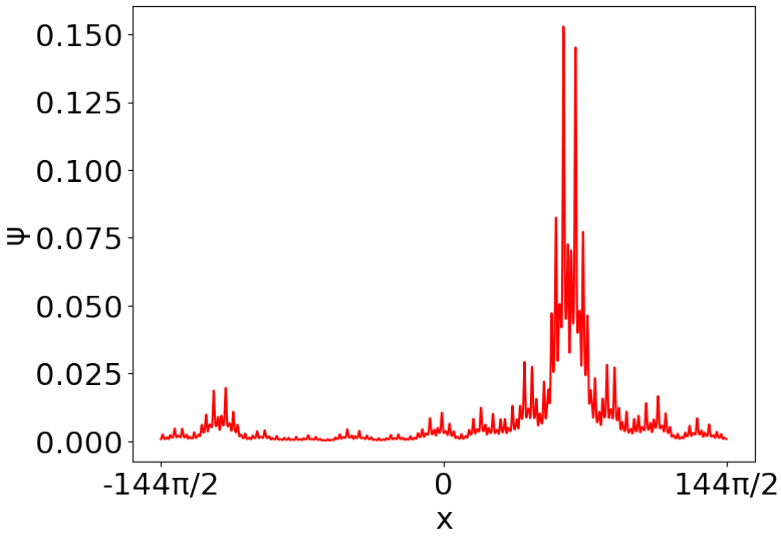

Figure 5.30: Localized perturbation for the stable state from Figure 5.27.

This perturbation is again localized, which means that we found what we were looking for. Even though we used a nonlinear state with a chemical potential close to the Linear value, we calculated that the state presents strong nonlinearity. Now all that we need to look for is a localized soliton.

5.6.2.2 Soliton

In order to look for this type of localized excitation we can begin by looking at the states calculated in Figure 5.19. These states are unstable at a potential quite close to the linear one, which suggests that it may be easier to find localized excitations in these states. Looking for example at the nonlinear state with potential $\mu = -0.2160$, we have the Figure 5.31.

We see that the state is delocalized as intended, which means that we may proceed by calculating the Bogoliubov-de Gennes spectrum, which we can represent in the complex plane once again in Figure 5.32.

We see that there are excitations with an eigenvalue with a nonzero complex part, which shows us that the underlying state from Figure 5.31 is unstable. Now we must conclude whether the excitation associated to the eigenvalue with the largest imaginary part ($\omega = 0.003209i$) is localized or not. Representing that excitation we obtain Figure 5.33.

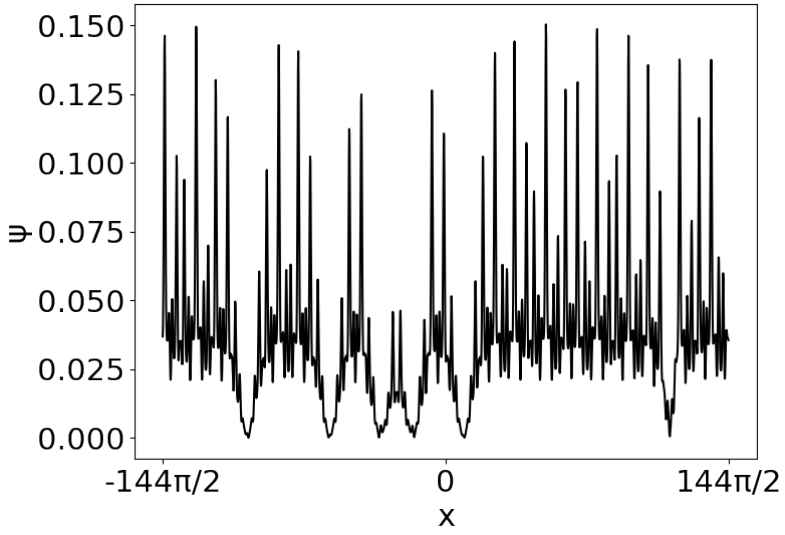

Figure 5.31: Nonlinear state for a Repulsive particle interaction, amplitudes $v_1 = 0.8; v_2 = 0.65$ and chemical potential $\mu = -0.2160$ calculated in Figure 5.15

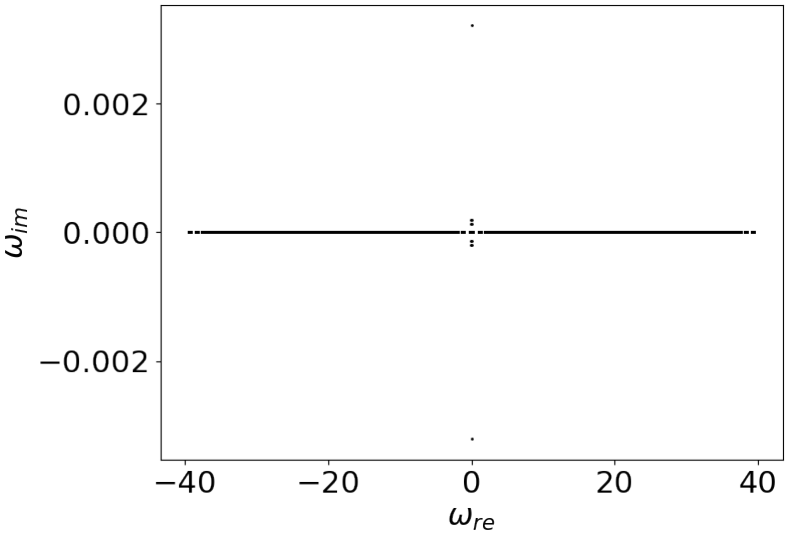

Figure 5.32: Spectrum of the Bogoliubov-de Gennes excitations for Figure 5.31. This spectrum has eigenvalues that are imaginary, meaning that the state from Figure 5.31 is unstable.

And we see again that we have obtained a localized excitation from a delocalized state, this time a soliton that we will want to propagate in time in order to better observe the dynamical stability of the condensate and confirm the validity of the analysis we are performing.

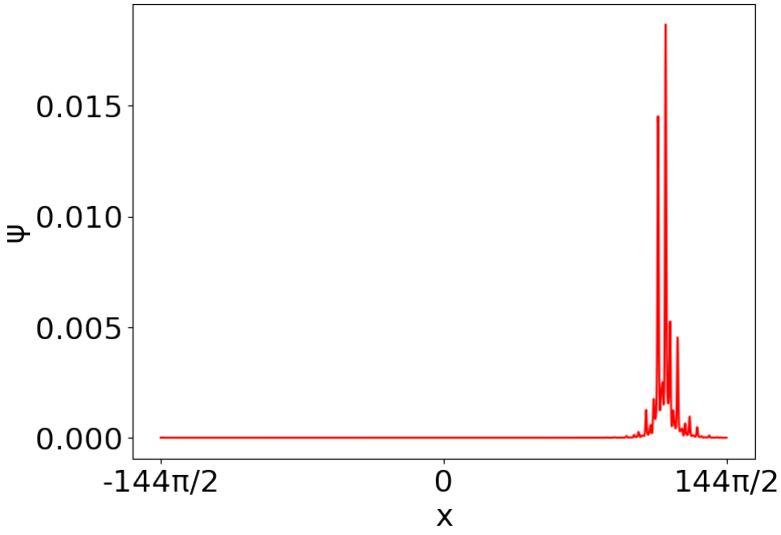

Figure 5.33: Localized perturbation for the unstable state from Figure 5.31.

5.7 Time Evolution

In this final section we want to take the states we calculated to be unstable, perturb them with the localized excitations we calculated and analyze their temporal propagation, in order to probe the timescale of the instability of the Condensate. Let's begin by calculating this evolution for the Condensate with an Attractive particle interaction.

5.7.1 Attractive Interaction

We are going to take the state represented in Figure 5.24 and perturb it by adding the state from Figure 5.26, and from that we are going to apply the time evolution algorithm detailed in the previous chapter. For the time evolution we are going to calculate how the Condensate evolves through 1000 time units with a time step $\Delta t = 5 \cdot 10^{-3}$. We want to check whether the condensate remains stable throughout this interval or if it decays away. The result obtained for these conditions is presented in Figure 5.34.

As can be seen in the figure, this timescale of evolution showcases the instability of the Condensate. For the first 600 time units the Condensate remains largely unaffected by the perturbation, and only after that timestamp we see it begin to decay away. This confirms what was expected from the results obtained via the Linear Stability Analysis. Another thing we might look at is if we define a "proper time", meaning a timescale for the stability of the condensate, as $\tau = \frac{1}{\omega_{im}}$, we can see that for this state we will have a proper time $\tau = \frac{1}{0.02689} \approx 37.19$, meaning that in this case the decay occurred at around

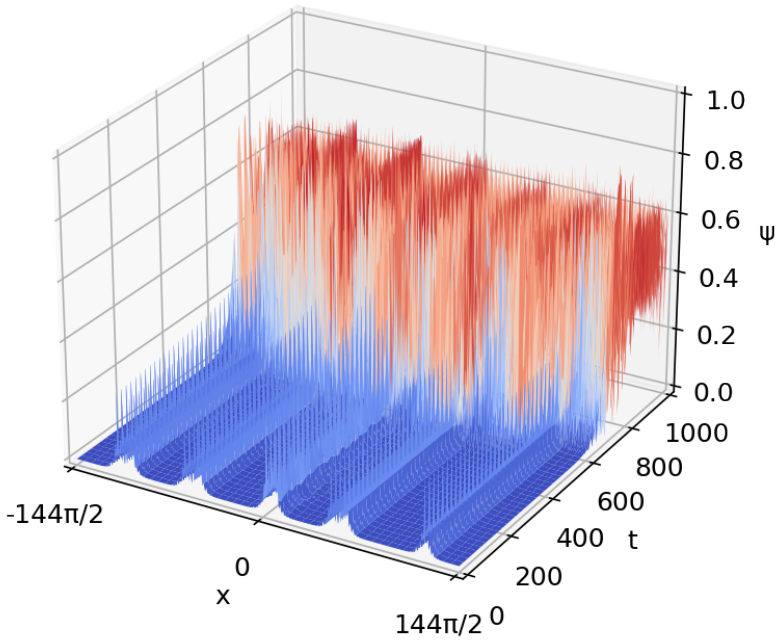

Figure 5.34: Time evolution of the Condensate with an Attractive interaction and potential amplitudes $v_1 = 0.8; v_2 = 0.3$ perturbed by the state from Figure 5.26

16.13τ. This value may be due to the size of the perturbation, where if we added a bigger one the condensate would decay faster.

5.7.2 Repulsive Interaction

Let's look now at the time evolution of the Condensate with a Repulsive particle interaction. Once again we propagate this system for 650 time units and with a time step of $\Delta t = 2.5 \cdot 10^{-3}$. We obtain the dynamic presented in Figure 5.35.

We see that similarly to our previous case the Condensate remains unchanged around the first 620 time units, and only after that we see the instability begin to manifest around the place where it was perturbed by the state from Figure 5.33. Once again the validity of the Linear Stability Analysis is confirmed. Defining again the proper time for this condensate, this time we will obtain the value $\tau = \frac{1}{0.0032} = 312.5$. Seeing as this time the condensate does not decay for 620 units of time, the timescale of this one is 1.98τ. Once again this value, although much smaller than in the previous case, probably arises from the size of the perturbation added.

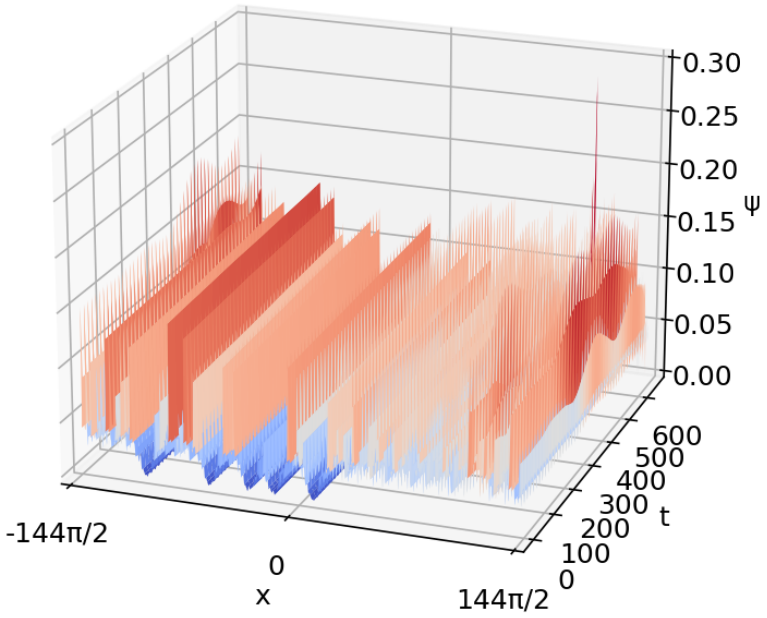

Figure 5.35: Time evolution of the Condensate with a Repulsive interaction and potential amplitudes $v_1 = 0.8; v_2 = 0.65$ perturbed by the state from Figure 5.33

Chapter 6

Conclusion

In this thesis we set out to to look at the effect that breaking the symmetry of a quasi periodic potential has on some properties of the non interacting BEC and to look for localized excitations rising from delocalized steady states of a repulsively or attractively interacting BEC. In the first part we saw that adding a phase difference to one of the constituent waves of the quasi periodic potential had no effect on the mobility edge of the condensate, seeing as it remained on the N^{th} state, where N comes from the rational approximation of the golden ratio $\varphi \approx \frac{M}{N}$. Another property that remained unchanged was the memory effect of the condensate, manifested by the energy gaps present at the levels whose number can be used to calculate a rational approximation of φ. The fact that these properties remain unchanged is to be expected, since they are entirely dependent on a parameter that was not changed by breaking this symmetry, the rational approximation. It was also seen that the symmetry of the left and right centers of mass of the condensate is broken, and this makes sense since it was dependent on the underlying symmetry of the potential.

When we moved on to the matter waves we were able to identify a mobility edge of the ground state of the non interacting condensate for the amplitude of the potentials, more specifically at $v_1 = 0.8, \quad v_2 = 0.6$. This transition made it so we were able to control with much better precision the size of the condensate by adjusting the amplitudes. This control became relevant as we added particle interactions, since we previously observed that the condensate expands when the interaction energy grows for a repulsive particle interaction and that it shrinks when the energy of an attractive particle interaction grows. From the delocalized nonlinear states obtained following this logic the linear stability analysis showed different results. For the condensates with attractive particle interaction a clear

tendency can be seen, where for one of the cases presented there is a transition from unstable to stable states. The other case presented tends asymptotically to stability. For the condensates with a repulsive particle interaction the behaviour is quite different, as for in both cases presented the condensate alternates between stable and unstable. This behaviour may be due to the fact that the potential amplitudes used for this case stand around the mobility edge, and it would perhaps be interesting to further investigate the stability of these condensates around the mobility edge. Nevertheless we were able to obtain localized excitations for each type of particle interaction, both stable and unstable. For the stable states it was found that the perturbations with the highest value of the IPR (meaning smaller size) corresponded to an eigenvalue of zero. For the unstable states a similar thing occurred, where these states had a zero real part of the eigenvalue, but a nonzero imaginary part, since that is what characterizes an unstable state. For the states we deemed unstable we also calculated the time frame of their stability. For the condensate with attractive particle interaction this time frame was around 600 units of time, which corresponds to 16.13τ looking at it in terms of the proper time, whereas for the repulsive condensate this value was 620 units of time, which corresponds to just 1.98τ. These values are quite different and represent different dynamics of these specific states. They might also be dependant on the size of the perturbation added. One potential study might also be to try and relate the size of the perturbation added to the steady state of the condensate and the time frame of stability.

Bibliography

[1] V. M. Perez-Garcia, H. Michinel, and H. Herrero, "Bose–Einstein solitons in highly asymmetric traps," Physical Review A, vol. 57, no. 5, pp. 3837–3842, May 1998, arXiv:quant-ph/9803038. [Online]. Available: http://arxiv.org/abs/quant-ph/9803038 [Cited on pages 1, 3, and 6.]

[2] S. Burger, K. Bongs, S. Dettmer, W. Ertmer, K. Sengstock, A. Sanpera, G. V. Shlyapnikov, and M. Lewenstein, "Dark Solitons in Bose-Einstein Condensates," Physical Review Letters, vol. 83, no. 25, pp. 5198–5201, Dec. 1999, arXiv:cond-mat/9910487. [Online]. Available: http://arxiv.org/abs/cond-mat/9910487 [Cited on page 4.]

[3] A. Trombettoni and A. Smerzi, "Discrete Solitons and Breathers with Dilute Bose-Einstein Condensates," Physical Review Letters, vol. 86, no. 11, pp. 2353–2356, Mar. 2001. [Online]. Available: https://link.aps.org/doi/10.1103/PhysRevLett.86.2353

[4] A. A. Sukhorukov, "Enhanced soliton transport in quasi-periodic lattices with short-range aperiodicity," Physical Review Letters, vol. 96, no. 11, p. 113902, Mar. 2006, arXiv:nlin/0507027. [Online]. Available: http://arxiv.org/abs/nlin/0507027

[5] K. E. Strecker, G. B. Partridge, A. G. Truscott, and R. G. Hulet, "Bright matter wave solitons in Bose–Einstein condensates," New Journal of Physics, vol. 5, pp. 73–73, Jun. 2003. [Online]. Available: https://iopscience.iop.org/article/10.1088/1367-2630/5/1/373

[6] ——, "Formation and propagation of matter-wave soliton trains," Nature, vol. 417, no. 6885, pp. 150–153, May 2002. [Online]. Available: https://www.nature.com/articles/nature747 [Cited on page 4.]

[7] L. Khaykovich, F. Schreck, G. Ferrari, T. Bourdel, J. Cubizolles, L. D. Carr, Y. Castin, and C. Salomon, "Formation of a Matter-Wave Bright Soliton,"

Science, vol. 296, no. 5571, pp. 1290–1293, May 2002. [Online]. Available: https://www.science.org/doi/10.1126/science.1071021 [Cited on page 4.]

[8] T. Busch and J. R. Anglin, "Mossbauer effect for dark solitons in Bose-Einstein condensates," Sep. 1998, arXiv:cond-mat/9809408. [Online]. Available: http://arxiv.org/abs/cond-mat/9809408 [Cited on page 4.]

[9] J. T. Mendonça, F. Haas, and A. Gammal, "Nonlinear vortex-phonon interactions in a Bose–Einstein condensate," Journal of Physics B: Atomic, Molecular and Optical Physics, vol. 49, no. 14, p. 145302, Jul. 2016. [Online]. Available: https://iopscience.iop.org/article/10.1088/0953-4075/49/14/145302

[10] I. Danaila, M. A. Khamehchi, V. Gokhroo, P. Engels, and P. G. Kevrekidis, "Vector Dark-Antidark Solitary Waves in Multi-Component Bose-Einstein condensates," Physical Review A, vol. 94, no. 5, p. 053617, Nov. 2016, arXiv:1606.05607 [cond-mat, physics:nlin]. [Online]. Available: http://arxiv.org/abs/1606.05607

[11] B. P. Anderson, P. C. Haljan, C. A. Regal, D. L. Feder, L. A. Collins, C. W. Clark, and E. A. Cornell, "Watching Dark Solitons Decay into Vortex Rings in a Bose-Einstein Condensate," Physical Review Letters, vol. 86, no. 14, pp. 2926–2929, Apr. 2001. [Online]. Available: https://link.aps.org/doi/10.1103/PhysRevLett.86.2926 [Cited on page 1.]

[12] A. Einstein, "Quantentheorie des einatomigen idealen gasen," Journal of the Prussian Academy of Sciences and Humanities, 1925. [Cited on page 3.]

[13] Bose, "Plancks Gesetz und Lichtquantenhypothese," Zeitschrift f r Physik, vol. 26, no. 1, pp. 178–181, Dec. 1924. [Online]. Available: http://link.springer.com/10.1007/BF01327326 [Cited on page 3.]

[14] M. H. Anderson, J. R. Ensher, M. R. Matthews, C. E. Wieman, and E. A. Cornell, "Observation of bose-einstein condensation in a dilute atomic vapor," Science, vol. 269, no. 5221, pp. 198–201, 1995. [Online]. Available: https://www.science.org/doi/abs/10.1126/science.269.5221.198 [Cited on page 3.]

[15] F. Dalfovo, S. Giorgini, L. P. Pitaevskii, and S. Stringari, "Theory of Bose-Einstein condensation in trapped gases," Reviews of Modern Physics, vol. 71, no. 3, pp. 463–512, Apr. 1999, arXiv:cond-mat/9806038. [Online]. Available: http://arxiv.org/abs/cond-mat/9806038 [Cited on page 3.]

[16] C. W. Gardiner, "A particle-number-conserving Bogoliubov method which demonstrates the validity of the time-dependent Gross-Pitaevskii equation for a highly condensed Bose gas," Physical Review A, vol. 56, no. 2, pp. 1414–1423, Aug. 1997, arXiv:quant-ph/9703005. [Online]. Available: http://arxiv.org/abs/quant-ph/9703005 [Cited on pages 4 and 5.]

[17] C. Pethick and H. Smith, Bose-Einstein condensation in dilute gases. Cambridge ; New York: Cambridge University Press, 2002. [Cited on page 5.]

[18] P. J. Y. Louis, E. A. Ostrovskaya, C. M. Savage, and Y. S. Kivshar, "Bose-Einstein Condensates in Optical Lattices: Band-Gap Structure and Solitons," Physical Review A, vol. 67, no. 1, p. 013602, Jan. 2003, arXiv:cond-mat/0208516. [Online]. Available: http://arxiv.org/abs/cond-mat/0208516 [Cited on pages 7 and 10.]

[19] N. Wiener, "A New Definition of Almost Periodic Functions," The Annals of Mathematics, vol. 28, no. 1/4, p. 365, 1926. [Online]. Available: https://www.jstor.org/stable/1968381?origin=crossref [Cited on page 10.]

[20] D. Levine and P. J. Steinhardt, "Quasicrystals: A New Class of Ordered Structures," Physical Review Letters, vol. 53, no. 26, pp. 2477–2480, Dec. 1984. [Online]. Available: https://link.aps.org/doi/10.1103/PhysRevLett.53.2477 [Cited on page 12.]

[21] Y. Cao, V. Fatemi, S. Fang, K. Watanabe, T. Taniguchi, E. Kaxiras, and P. Jarillo-Herrero, "Unconventional superconductivity in magic-angle graphene superlattices," Nature, vol. 556, no. 7699, pp. 43–50, Apr. 2018. [Online]. Available: https://www.nature.com/articles/nature26160 [Cited on page 12.]

[22] P. W. Anderson, "Absence of Diffusion in Certain Random Lattices," Physical Review, vol. 109, no. 5, pp. 1492–1505, Mar. 1958. [Online]. Available: https://link.aps.org/doi/10.1103/PhysRev.109.1492 [Cited on page 12.]

[23] S. K. Adhikari and L. Salasnich, "Localization of a Bose-Einstein condensate in a bichromatic optical lattice," Physical Review A, vol. 80, no. 2, p. 023606, Aug. 2009, arXiv:0907.3498 [cond-mat]. [Online]. Available: http://arxiv.org/abs/0907.3498 [Cited on page 12.]

[24] S. E. Skipetrov, A. Minguzzi, B. A. van Tiggelen, and B. Shapiro, "Anderson localization of a Bose-Einstein condensate in a 3D random potential," Physical

Review Letters, vol. 100, no. 16, p. 165301, Apr. 2008, arXiv:0801.3631 [cond-mat]. [Online]. Available: http://arxiv.org/abs/0801.3631 [Cited on page 12.]

[25] G. Roati, C. D'Errico, L. Fallani, M. Fattori, C. Fort, M. Zaccanti, G. Modugno, M. Modugno, and M. Inguscio, "Anderson localization of a non-interacting Bose–Einstein condensate," Nature, vol. 453, no. 7197, pp. 895–898, Jun. 2008. [Online]. Available: https://www.nature.com/articles/nature07071 [Cited on page 12.]

[26] G. Roati, M. Zaccanti, C. D'Errico, J. Catani, M. Modugno, A. Simoni, M. Inguscio, and G. Modugno, "39-K Bose-Einstein condensate with tunable interactions," Physical Review Letters, vol. 99, no. 1, p. 010403, Jul. 2007, arXiv:cond-mat/0703714. [Online]. Available: http://arxiv.org/abs/cond-mat/0703714 [Cited on page 12.]

[27] S. Ray, M. Pandey, A. Ghosh, and S. Sinha, "Localization of weakly interacting Bose gas in quasiperiodic potential," New Journal of Physics, vol. 18, no. 1, p. 013013, Dec. 2015. [Online]. Available: https://iopscience.iop.org/article/10.1088/1367-2630/18/1/013013 [Cited on page 12.]

[28] Y. Lahini, R. Pugatch, F. Pozzi, M. Sorel, R. Morandotti, N. Davidson, and Y. Silberberg, "Observation of a localization transition in quasiperiodic photonic lattices," Phys. Rev. Lett., vol. 103, p. 013901, Jun 2009. [Online]. Available: https://link.aps.org/doi/10.1103/PhysRevLett.103.013901 [Cited on page 12.]

[29] B. Hu, G. Huang, and Y.-l. Ma, "Analytical solutions of the Bogoliubov–de Gennes equations for excitations of a trapped Bose-Einstein-condensed gas," Physical Review A, vol. 69, no. 6, p. 063608, Jun. 2004. [Online]. Available: https://link.aps.org/doi/10.1103/PhysRevA.69.063608 [Cited on page 21.]

[30] P. Pieri and G. C. Strinati, "Derivation of the Gross-Pitaevskii Equation for Condensed Bosons from the Bogoliubov–de Gennes Equations for Superfluid Fermions," Physical Review Letters, vol. 91, no. 3, p. 030401, Jul. 2003. [Online]. Available: https://link.aps.org/doi/10.1103/PhysRevLett.91.030401 [Cited on page 21.]

[31] W. Bao and Y. Cai, "Mathematical theory and numerical methods for Bose-Einstein condensation," Kinetic & Related Models, vol. 6, no. 1, pp. 1–135, 2013,

arXiv:1212.5341 [cond-mat]. [Online]. Available: http://arxiv.org/abs/1212.5341 [Cited on page 21.]

[32] E. Kengne and R. Vaillancourt, "Exact solutions of the Gross-Pitaevskii equation in periodic potential in the presence of external source," Journal of Mathematical Physics, vol. 48, no. 7, p. 073520, Jul. 2007. [Online]. Available: https://pubs.aip.org/jmp/article/48/7/073520/912146/Exact-solutions-of-the-Gross-Pitaevskii-equation [Cited on page 24.]

[33] H. C. Prates, D. A. Zezyulin, and V. V. Konotop, "Bose-Einstein condensates in quasi-periodic lattices: bosonic Josephson junction, self-trapping, and multi-mode dynamics," Aug. 2022, arXiv:2208.10376 [cond-mat, physics:nlin, physics:physics]. [Online]. Available: http://arxiv.org/abs/2208.10376 [Cited on pages 29, 30, and 33.]